USGS
science for a changing world

Reconnaissance Borehole Geophysical, Geological, and Hydrological Data from the Proposed Hydrodynamic Compartments of the Culpeper Basin in Loudoun, Prince William, Culpeper, Orange, and Fairfax Counties, Virginia [Version 1.0]

By Michael P. Ryan, Herbert A. Pierce, Carole D. Johnson, David M. Sutphin, David L. Daniels, Joseph P. Smoot, John K. Costain, Cahit Çoruh, and George E. Harlow

Open–File Report 2006-1203

U.S. Department of the Interior
U.S. Geological Survey

Reconnaissance Borehole Geophysical, Geological, and Hydrological Data from the Proposed Hydrodynamic Compartments of the Culpeper Basin in Loudoun, Prince William, Culpeper, Orange, and Fairfax Counties, Virginia [Version 1.0]

By Michael P. Ryan, Herbert A. Pierce, Carole D. Johnson, David M. Sutphin, David L. Daniels, Joseph P. Smoot, John K. Costain, Cahit Çoruh, and George E. Harlow

Open-File Report 2006–1203

U.S. Department of the Interior
U.S. Geological Survey

U.S. Department of the Interior
DIRK KEMPTHORNE, Secretary

U.S. Geological Survey
Mark D. Meyers, Director

U.S. Geological Survey, Reston, Virginia: 2007

For product and ordering information:
World Wide Web: http://www.usgs.gov/pubprod
Telephone: 1-888-ASK-USGS

For more information on the USGS--the Federal source for science about the Earth, its natural and living resources, natural hazards, and the environment:
World Wide Web: http://www.usgs.gov
Telephone: 1-888-ASK-USGS

Suggested citation:
Ryan, Michael P., Pierce, Herbert A., Johnson, Carole D., Sutphin, David M., Daniels, David L., Smoot, Joseph P., Costain, John K., Çoruh, Cahit, and Harlow, George E., 2007, Reconnaissance borehole geophysical, geological and hydrological data from the proposed hydrodynamic compartments of the Culpeper Basin in Loudoun, Prince William, Culpeper, Orange and Fairfax Counties, Virginia. [Version 1.0]: U.S. Geological Survey Open File Report 2006-1203, 43p.

2001051109

ISBN 978-1-4113-2031-4

Contents

Figures

Tables

Conversion Factors

Multiply	By	To obtain
	Length	
inch (in.)	2.54	centimeter (cm)
inch (in.)	25.4	millimeter (mm)
foot (ft)	0.3048	meter (m)
mile (mi)	1.609	kilometer (km)
yard (yd)	0.9144	meter (m)
	Area	
square foot (ft^2)	929.0	square centimeter (cm^2)
square foot (ft^2)	0.09290	square meter (m^2)
square inch (in^2)	6.452	square centimeter (cm^2)
square mile (mi^2)	259.0	hectare (ha)
square mile (mi^2)	2.590	square kilometer (km^2)
	Volume	
ounce, fluid (fl. oz)	0.02957	liter (L)
pint (pt)	0.4732	liter (L)
quart (qt)	0.9464	liter (L)
gallon (gal)	3.785	liter (L)
gallon (gal)	0.003785	cubic meter (m^3)
gallon (gal)	3.785	cubic decimeter (dm^3)
cubic inch (in^3)	16.39	cubic centimeter (cm^3)
cubic inch (in^3)	0.01639	cubic decimeter (dm^3)
cubic inch (in^3)	0.01639	liter (L)
cubic foot (ft^3)	28.32	cubic decimeter (dm^3)
cubic foot (ft^3)	0.02832	cubic meter (m^3)
cubic yard (yd^3)	0.7646	cubic meter (m^3)
cubic mile (mi^3)	4.168	cubic kilometer (km^3)
	Flow rate	
foot per second (ft/s)	0.3048	meter per second (m/s)
foot per minute (ft/min)	0.3048	meter per minute (m/min)
foot per hour (ft/hr)	0.3048	meter per hour (m/hr)
foot per day (ft/d)	0.3048	meter per day (m/d)
foot per year (ft/yr)	0.3048	meter per year (m/yr)
cubic foot per second (ft^3/s)	0.02832	cubic meter per second (m^3/s)
cubic foot per day (ft^3/d)	0.02832	cubic meter per day (m^3/d)
gallon per minute (gal/min)	0.06309	liter per second (L/s)
gallon per day (gal/d)	0.003785	cubic meter per day (m^3/d)
million gallons per day (Mgal/d)	0.04381	cubic meter per second (m^3/s)
	Mass	
ounce, avoirdupois (oz)	28.35	gram (g)
pound, avoirdupois (lb)	0.4536	kilogram (kg)
	Pressure	
atmosphere, standard (atm)	101.3	kilopascal (kPa)
bar	100	kilopascal (kPa)
inch of mercury at 60ºF (in. Hg)	3.377	kilopascal (kPa)
pound-force per square inch (lbf/in^2)	6.895	kilopascal (kPa)
pound-force per square foot (lbf/ft^2)	0.04788	kilopascal (kPa)
	Density	
pound per cubic foot (lb/ft^3)	16.02	kilogram per cubic meter (kg/m^3)
pound per cubic foot (lb/ft^3)	0.01602	gram per cubic centimeter (g/cm^3)
	Energy	
kilowatthour (kWh)	3,600,000	joule (J)
	Radioactivity	
picocurie per liter (pCi/L)	0.037	becquerel per liter (Bq/L)

	Specific capacity	
gallon per minute per foot [(gal/min)/ft)]	0.2070	liter per second per meter [(L/s)/m]
	Hydraulic conductivity	
foot per day (ft/d)	0.3048	meter per day (m/d)
	Hydraulic gradient	
foot per mile (ft/mi)	0.1894	meter per kilometer (m/km)
	Transmissivity*	
foot squared per day (ft^2/d)	0.09290	meter squared per day (m^2/d)
	Application rate	
	Leakance	
foot per day per foot [(ft/d)/ft]	1	meter per day per meter
inch per year per foot [(in/yr)/ft]	83.33	millimeter per year per meter [(mm/yr)/m]

Temperature in degrees Celsius (°C) may be converted to degrees Fahrenheit (°F) as follows:

$$°F=(1.8\times°C)+32$$

Temperature in degrees Fahrenheit (°F) may be converted to degrees Celsius (°C) as follows:

$$°C=(°F-32)/1.8$$

Vertical coordinate information is referenced to the North American Vertical Datum of 1988 (NAVD 88).

Horizontal coordinate information is referenced to the North American Datum of 1927 (NAD 27)."

Altitude, as used in this report, refers to distance above the vertical datum.

*Transmissivity: The standard unit for transmissivity is cubic foot per day per square foot times foot of aquifer thickness [(ft^3/d)/ft^2]ft. In this report, the mathematically reduced form, foot squared per day (ft^2/d), is used for convenience.

Specific conductance is given in microsiemens per centimeter at 25 degrees Celsius (µS/cm at 25 °C).

Concentrations of chemical constituents in water are given either in milligrams per liter (mg/L) or micrograms per liter (µg/L).

Reconnaissance Borehole Geophysical, Geological, and Hydrological Data from the Proposed Hydrodynamic Compartments of the Culpeper Basin in Loudoun, Prince William, Culpeper, Orange, and Fairfax Counties, Virginia [Version 1.0]

By Michael P. Ryan, Herbert A. Pierce, Carole D. Johnson, David M. Sutphin, David L. Daniels, Joseph P. Smoot, John K. Costain, Cahit Çoruh, and George E. Harlow

Abstract and Summary of Select Structural Results Within a Culpeper Basin Context

A range of geophysical borehole tools have allowed the measurements of both fluid and petrophysical properties of fluid-saturated sedimentary and igneous rocks within an eastern North American rift zone basin. These measurements include: the fluid temperature-depth function ($T-Z$) and the first spatial derivative of temperature, ($\frac{DT}{DZ}$); the formation electrical conductivity ($\sigma_{formation}$) and resistivity ($\rho_{formation}$); the fluid conductivity (σ_{fluid}) and resistivity (ρ_{fluid}); the natural gamma count (Γ) and the variations in borehole diameter (Δr) via caliper data. In addition, Optical TeleViewer (OTV) and Acoustic TeleViewer (ATV) logging, as well as heat pulse and E-M flowmeter logging has also been conducted. Not all boreholes discussed in this report were logged with the entire suite of tools.

The resulting program of borehole geophysical surveys has been conducted in the Mesozoic Culpeper basin of Virginia. Ryan and others, (2007a, b), present the primary evidence that the Culpeper basin is hydrodynamically compartmentalized. The results of this report are both consistent with the compartmentalization concept, and offer further elaboration of how compartments are internally structured. While complimenting the reports cited above, these results do not, however, provide definitive evidence for the proposed compartmentalization concept. The principal results of individual surveys are organized on a structural basis. **The Dulles compartment**. Two wells have been logged, and both are sited wholly within the Balls Bluff Siltstone. In Dulles Well No. 2 (total depth = 289 m) thirty three spikes in the first derivative of temperature with respect to depth, $\frac{DT}{DZ}$, are consistent with the inflow of groundwater from a multiplicity of fractures that intersect the borehole. The spikes are unevenly distributed with depth, however they are broadly consistent with the spacing between bedding plane fractures within the Balls Bluff Member of the Bull Run Formation. **The Gainesville compartment**. Direct drilling has been conducted through the Gainesville diabase sheet into the subjacent hornfels (thermally metamorphosed after Balls Bluff Member siltstone). The diabase-hornfels interface (at a depth of 183 m) represents a basal flow regime where the hornfels comprises the permeable top of the Gainesville compartment confined by the diabase above. Total hole depth is 226 m. Optical TeleViewer (OTV) logging reveals that the transition from diabase to hornfels is characterized by moderate fracturing within the diabase and a massively fractured hornfels beneath. Driller's pumped flow rates within the diabase are ~2 gallons per minute (gpm), whereas flow rates within the hornfels at the compartment top are ~110+ gpm. These results offer further evidence supporting the compartmentalization concept. In this context, basal flow occurs within the hornfels that immediately underlies the less permeable diabase confining unit. **The Rapidan compartment**. Five boreholes at the Coffeewood Correctional Center near Mitchells, Virginia have been logged to determine the relationships between the hornfels (thermally metamorphosed after Balls Bluff Member siltstone) and the diabase beneath. The transition from hornfels to diabase (the structure of the compartment base) is particularly notable in the natural gamma counts where, in well OBS–5, a complete disappearance of gamma counts occurs at a depth of 107.5 m. Paleoflow inferences include the marked increases that occur in calcite vein frequency between 72 and 104 m. Calcite veins die out, however, dramatically above 70 m suggesting that the lower 32 m of hornfels immediately above the diabase experienced intense hydrothermal circulation during the cooling of the lopolith. Pre-logging pumping tests conducted in well OBS–4 proximal to the underlying Rapidan diabase lopolith induced exceptional drawdown suggesting the presence of a

low permeabilty barrier (diabase). These results are entirely consistent with—and can be best explained by—the compartmentalization of Rapidan fluids. **The structural eastern margin of the Culpeper basin**. The eastern edge of the basin displays an on-lap relationship between the Poolesville Member of the Manassas Sandstone and the Proterozoic basement schists. The basin-basement contact and the overlying sediments dip about 10 degrees westward. Interbedded sandstones and siltstones comprise the Upper Triassic Manassas Sandstone, and these grade downwards into the conglomerate of the Reston Conglomerate (forming the base below the Manassas Sandstone). The Reston Conglomerate lies unconformably on the partially weathered Proterozoic schists of the underlying basement. In well 52V–2D, pumping tests induced inflow to the well bore from three separate depth levels resulting in a net upward flow polarity for the well. Sites of inflow have been correlated with bedding plane fractures within the Manassas Sandstone. This well has a transmissivity, *T*, of 44 x 10^{-4} to 47 x 10^{-5} ft^2/day and a storativity, *S*, of 1 x 10^{-4} to 6 x 10^{-5}.

Introduction

The Culpeper basin is part of a much larger system of ancient depressions or troughs, that lie inboard of the Atlantic Coastal Plain, and largely within the Applachian Piedmont Geologic Province of eastern North America, and the transition region with the neighboring Blue Ridge Geologic Province. This basin system formed during an abortive attempt to make a great ocean basin during the Late Triassic and Early Jurassic, and the eroded remnants of the basins record major episodes of sedimentation, igneous intrusion and eruption, and pervasive contact metamorphism. Altogether, some twenty nine basins formed between what is now Nova Scotia and Georgia. Many of these basins are discontinuous along their strike, and have therefore recorded isolated environments for fluvial and lacustrine sedimentation.

Several basins (including the Culpeper, Gettysburg, and Newark basins) are fault-bounded on the west, and Mesozoic crustal stretching has produced assymetrical patterns of basin subsidence resulting in a progressive basin deepening to the west, and a virtual onlap relationship with the pre-basin Proterozoic rocks to the east. A result of such a pattern of basin deepening is the development of sequences of sandstones and siltstones that systemmatically increase in dip towards the accomodating western border faults. A second major structural theme in several of the major Mesozoic basins (including the Culpeper) concerns the geometry of igneous intrusion, as discussed below. Froelich (1982, 1985) and Lee and Froelich (1989) discuss the general geology of the Culpeper basin, and Smoot (1989) discusses the sedimentation environments and sedimentary facies of the Mesozoic with respect to fluvial and shallow lacustrine deposition in the Culpeper basin. Ryan and others, 2007a, b, discuss the role of diabase-induced compartmentalization in the Culpeper basin (and other Mesozoic basins), and illustrate (using alteration mineral suites within the diabase and adjacent hornfels, among other evidence) how this process has played a role in organizing the paleo- and contemporary-flow of crustal fluids at local and regional scales. Within this report, the Newark Supergroup nomenclature of Weems and Olsen (1997) is adopted.

Motivation, Context and Purpose

We report here on the initial results from borehole geophysical surveys within the Culpeper basin. This is the first phase of a larger effort to compare and contrast the regional-to-local structural and lithologic features of Culpeper basin rocks that promote (or inhibit) the storage and transmission of groundwater. The selection of well locations was guided by these factors: (i) position within geologic units representing mayor sedimentary and/or structural features within the basin; (ii) appreciable depth of well, such that a significant sampling interval was possible; (iii) reasonable geographic distributions of wells; and (iv) boreholes within a significant 'basin-structural' and/or 'cultural' context. In this last category, the wells at the U.S. Geological Survey National Center campus sample the extreme eastern edge structure of the basin, whereas wells within the Dulles International Airport are positioned within a central region of the airport and the proposed Dulles hydrodynamic compartment. The purpose of the report is to develop a geological, petrophysical and meter-scale hydrological picture of the sandstone and siltstone contents of the basin's hydrodynamic compartments, the hornfels that comprises the compartment margins, and the diabase that comprises the compartment seals.

The purpose of the report is not, however, to establish the basis for the proposed compartmentalization concept. That basis has been presented in abstracts (Ryan and others, 1997, 2000, 2002) and is presented in two related companion papers by Ryan and others (2007a, b), among other reports, although we do briefly summarize certain aspects of that basis here. Several of the borehole results of this report, however, are very consistent with—and are optimally explained by the compartmentalization mechanism. Therefore our results are placed within the compartmentalization context, within which, we think, they can be better understood. It is expected that the reports of Ryan and others, 2007a, b may be read in conjunction with this report. In addition, the report of Ryan and others, (2007c) presents magnetotelluric (MT) survey results at basin-scale that describe the cross-sectional geometry of the basin and intra-basin compartments defined by diabase bodies.

Organization

We have tried to prepare a report that will be of use to those with backgrounds in geology, geophysics and hydrology. So that the report can be more accessable to this larger community, results are first prefaced by introductory summaries on aspects of regional geology and geophysics. These summaries

include the areal geology of the Culpeper basin, the digital topography, regional aeromagnetic anomaly distributions and the limited structural inferences drawn from seismic reflection surveys. In these summaries, we attempt to paint a picture of our emerging image of the three-dimensional structure of the Culpeper basin. A brief summary of the proposed compartmentalization concept next illustrates our model of how and why fluids are stored and migrate in the subsurface, highlighting some of the principal evidence for the concept, as summarized from Ryan and others (2007a, 2007b). Next, the report discusses the borehole logging data on a compartment-by-compartment basis, including the proposed Dulles-, Gainesville- and Rapidan-compartments. Then, a summary of logging options is included in appendix I. Tables and graphs of borehole data for each locale are presented in appendix II. Culpeper basin borehole data file downloading instructions are given in appendix III. Access maps for each of those wells logged are included in Appendix IV on field logistics. Finally, appendix V provides a brief glossary of selected terms.

Geophysical and Geological Setting

Digital Topography of the Culpeper Basin.

The physiographic grain of eastern North America is dominated by the Appalachian Mountains, the Blue Ridge Geologic Province, the Piedmont Geologic Province, and their relationships with the Atlantic Coastal Plain and the Atlantic Ocean coastline. Figure 1 illustrates several of these relationships, and sets the Culpeper and Barboursville basins within the topography of the surrounding Piedmont. The grid for this view was assembled from 144 USGS 7.5 minute Digital Elevation Model (DEM) files. Terrain values were spaced at 30 meters. Oasis Montaj software by GeoSoft was used to create the grid and the display of the terrain and the related aeromagnetic map of this report. Terrain colors were assigned by a histogram equalization distribution function in which all color intervals receive approximately equal display area. Boundary lines for the Culpeper and Barboursville Early Mesozoic basins are shown as white lines (the center of fig. 1) and for the Atlantic Coastal Plain (the eastern part of the figure). The Culpeper basin is clearly lower in elevation than the surrounding Piedmont crystalline terrain. The highest topography within the basin is mostly along the western border fault. Elevations range from 370 to 60 meters above sea level across the basins. The surface and near-surface hydrology is influenced by flow down—or within—a regional hydraulic gradient that starts in the highlands of the bordering western mountains, and migrates towards the east and north (Laczniak and Zenone, 1985). Superposed on this regional trend are the strong influences of recharge and local and sub-regional drainage. Frequently the local groundwater divides are topographic highs supported by the resistant diabase bodies that form low permeability compartment walls at depth. The surface drainage from the Culpeper basin follows at least five major pathways eastward. The fine texture of parallel lines in the west-central part of the Culpeper basin (see fig. 1) is an area of low parallel ridges produced by the differential erosion of the upturned edges of sediments laid down in ancient, but now west-dipping lake beds, a pattern well-exposed along the Dulles Greenway between Dulles International Airport and the town of Leesburg, Virginia. The pattern is truncated by the smoother terrain over exposed diabase. The prominent lineament in the southwest corner of the map, southeast of these two basins, is the expression of the Mountain Run Fault.

The digital topography of the Loudoun County portion of the Culpeper basin is presented in figure 2. Figure 2 illustrates the contrasts in topography between the western highlands and the lowland regions of the basin, highlighting the distribution of diabase bodies, and the dendritic stream networks that drain the interior of the northern part of the basin.

Aeromagnetic Anomalies Originating from Within and Beneath the Culpeper Basin

Long-wavelength Anomalies and the Basin Substructure

Figure 3 illustrates the aeromagnetic anomalies of the Culpeper and Barboursville basins and surroundings, from the Blue Ridge Geologic Province eastward through the basins to, and sometimes beyond, the western margins of the Atlantic Coastal Plain. The grid of aeromagnetic data for the Culpeper basin map is composed of information from 20 separate airborne surveys acquired by the USGS and Virginia Division of Mineral Resources, and flown between 1948 and 1989 with widely varying flight line spacing.

Magnetic anomalies within the basin boundaries originate from two primary rock sources:

1) Intra-basin early Mesozoic diabase intrusions, with additional anomalies produced by associated thermally-metamorphosed sediments (hornfels) adjacent to the diabase, and by basalt flows of the same age; and

2) Paleozoic-to-Precambrian metamorphic rocks that form the crystalline basement beneath the basin.

Many of the basin-basement anomalies are continuous with those anomalies produced by exposed rock units outside the basin, thus permitting the source rocks to be identified. Several of these rock units produce anomalies with much larger amplitudes than the intra-basin anomalies. Where the two sets of anomalies are superimposed, separation may be possible based on wavelength. Long-wavelength anomalies are typically linked to deeper regional features in the Proterozoic basement, such as the Catoctin Formation, the Mather Gorge Formation and the Sykesville Formation.

Prominent anomalies are derived from low-oxidation state, magnetite-bearing metabasalts of the Catoctin Formation that are exposed in both limbs of the Blue Ridge anticlinorium. More oxidized, non-magnetic, hematite-bearing metabasalts

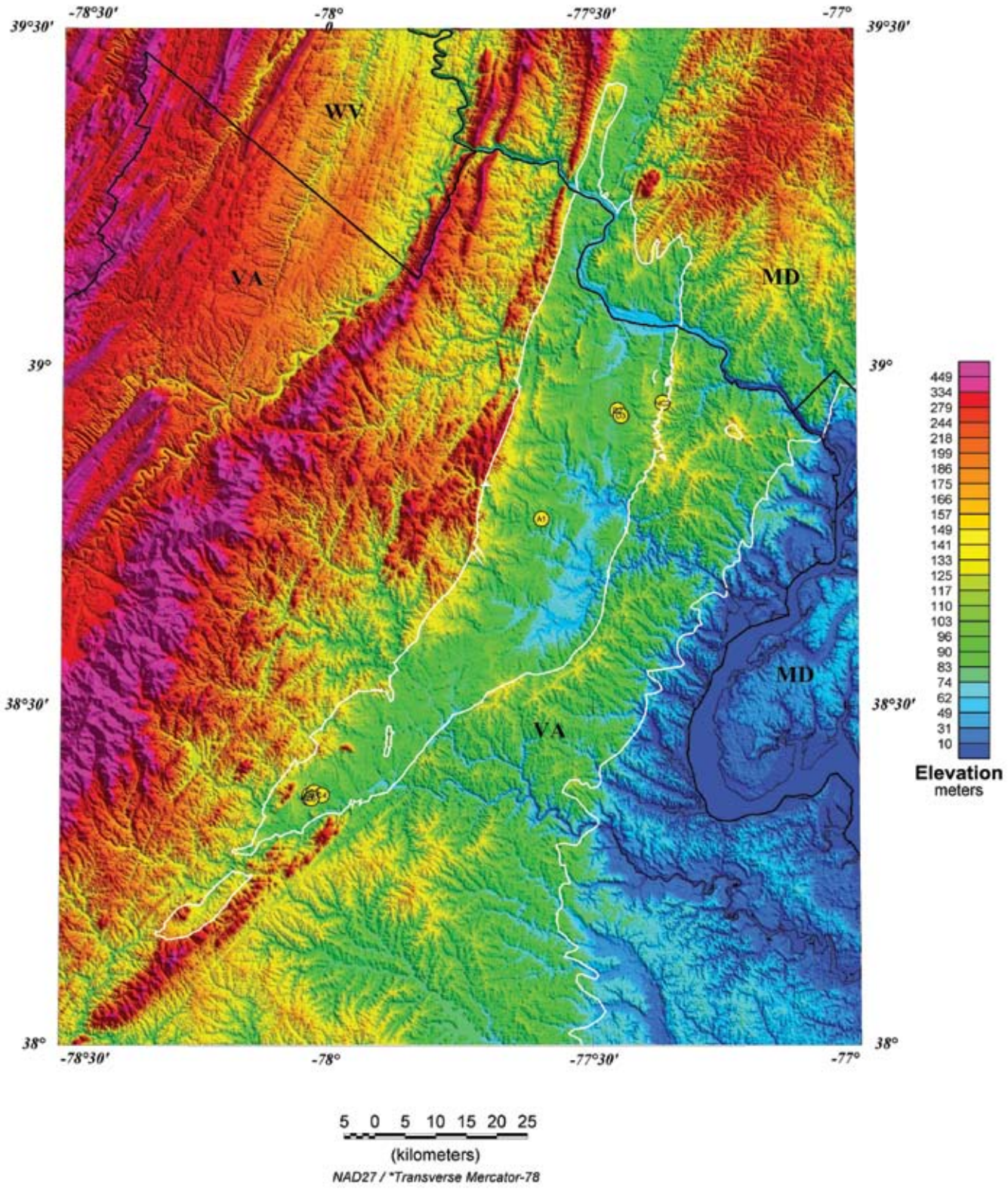

Figure 1. Digital terrain map of the Culpeper and Barboursville basins of Virginia and Maryland. The basin boundaries are outlined in white, with the relatively large Culpeper basin to the north of the more diminutive Barboursville. The position of the Atlantic Coastal Plain is the sutured-appearing white line in the southeast quadrant. The Blue Ridge Mountains dominate the landscape to the west and northwest. Major drainages are shown as deep blue dendritic patterns, and the Potomac River passes from northwest to southeast through the northern end of the basin. Borehole geophysical survey locations are indicated by yellow dots.

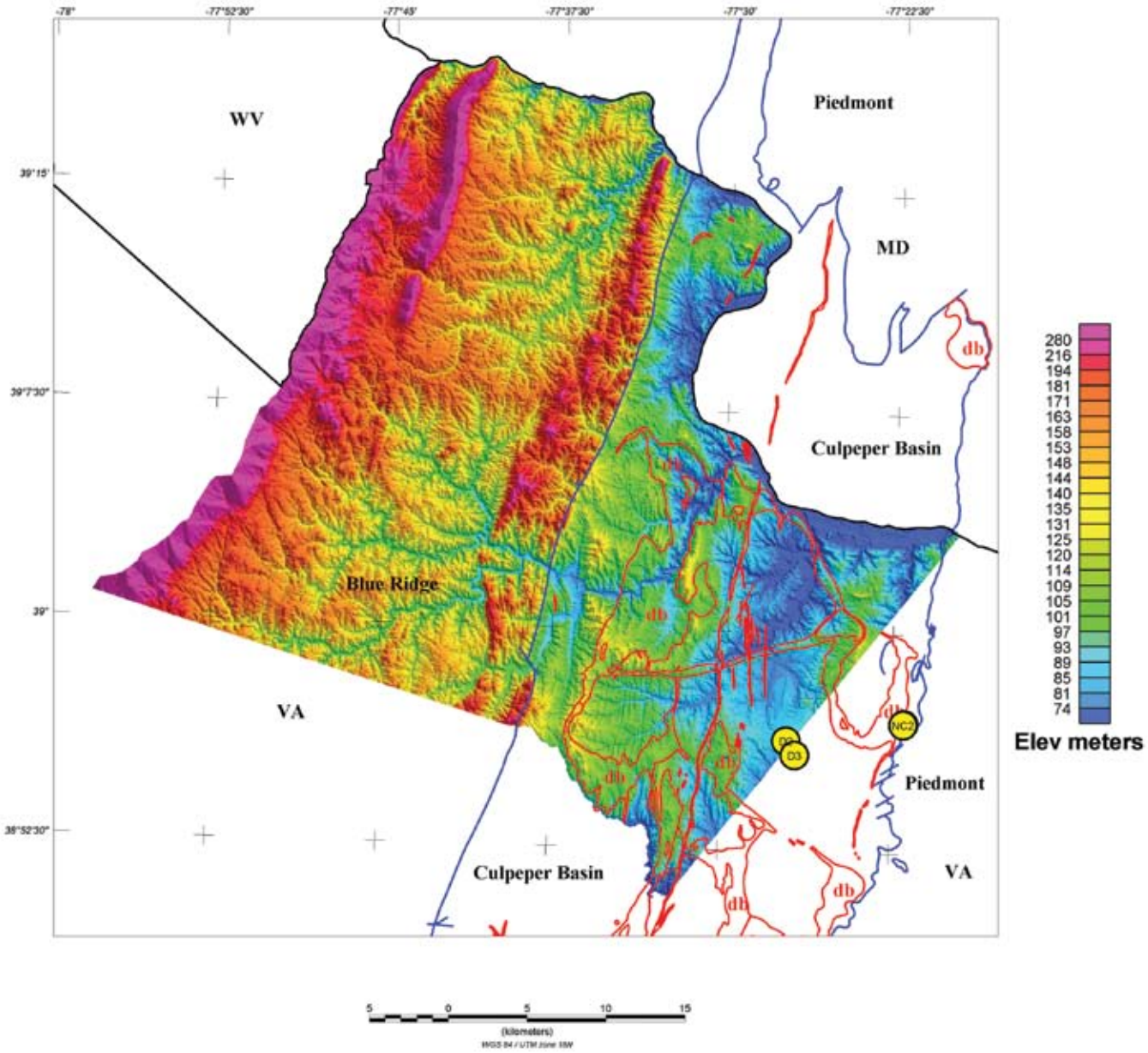

Figure 2. Digital terrain map of Loudoun County, Virginia. Outlines of the northern margin of the Culpeper basin are given in blue, whereas the outlines of the principal diabase bodies (central and eastern side of basin) are given in red (db). The diabase bodies are relatively low in permeability and effectively compartmentalize their surrounding sediments and metasediments with respect to fluid flow and storage. The sinusoidal contours of the northern margins of Loudoun County are defined by (and coincident with) the Potomac River (not labeled). Dendritic stream and river patterns in green illustrate the regional flow from west to east as well as into the Potomac River. The maroon spine of the northern Bull Run Mountains and Catoctin Mountain separates the Culpeper Basin in the eastern half of the figure from the Proterozoic geology in the west. Overall, relief spans the range 370 to 60 meters above mean sea level. Yellow dots denote the locations of borehole geophysical surveys at Dulles International Airport (western group of two locations) (D2, D3) and the U.S. Geological Survey National Center (NC2) (eastern-most location near the eastern margins of the Herndon diabase lopolith).

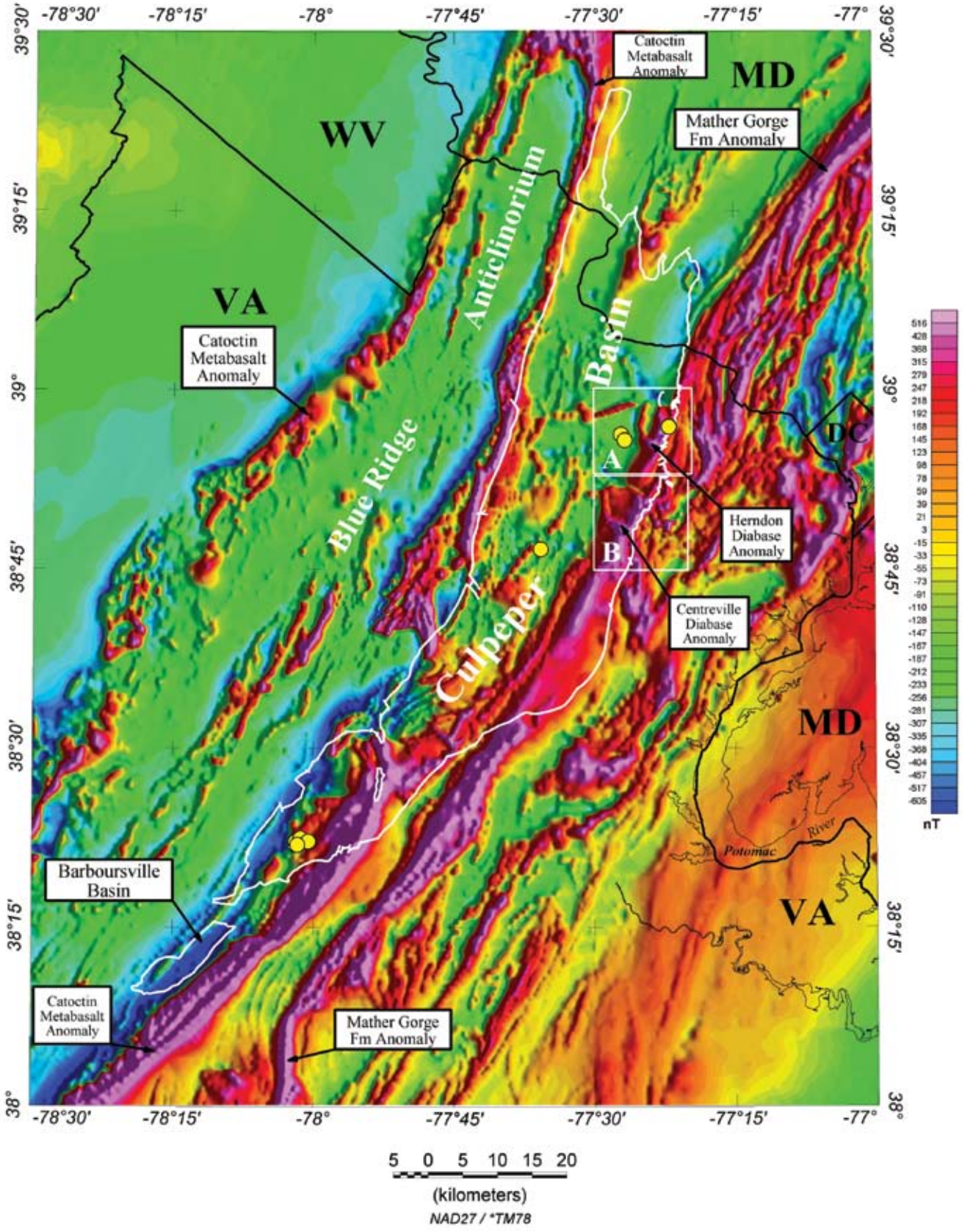
-78°30'
-78°15'
-78°
-77°45'
-77°30'
-77°15'
-77°
39°30'
39°15'
39°
38°45'
38°30'
38°15'
38°
WV
MD
VA
DC
Catoctin Metabasalt Anomaly
Mather Gorge Fm Anomaly
Blue Ridge
Anticlinorium
Culpeper
Basin
A
B
Herndon Diabase Anomaly
Centreville Diabase Anomaly
Barboursville Basin
Potomac River
nT
5 0 5 10 15 20
(kilometers)
NAD27 / *TM78

Figure 3. Aeromagnetic map of the Culpeper and Barboursville basins, showing the relationships between the magnetic anomalies and the major geologic and physiographic provinces of the region. Long wavelength anomalies include the 250 to 500 nT signature of the Catoctin metabasalt, that passes obliquely through the basement of the Culpeper basin, and lies just to the southeast of the Barboursville basin at those latitudes. An additional long wavelength anomaly is produced by the Mather Gorge Formation, which strikes NE-SW, and passes through the Culpeper basin basement in its east-central sector. The boundaries of the District of Columbia are given by the diamond-shaped box near the middle of the right-hand side of the figure. Yellow dots denote the locations of borehole geophysical survey locations. Boxes labled "A" and "B" denote the limits of figures 3*A* and 3*B*.

may make up more than half of the formation, depending on the area. Gravity is high over both classes of the metabasalt. The southeastern limb of this fold system lies west of the basin in the northern part of the area but crosses completely beneath the southwestern part of the Culpeper basin and re-appears on the southeast side of the basin.

Large-amplitude magnetic anomalies along the eastern edge of the basin reflect a broad band of quartz-rich metasediments in the Mather Gorge Formation and in the associated mélange of the Sykesville Formation; both of which may be Paleozoic in age (S. Southworth, pers. Comm.). The high magnetite content of these metasedimentary rocks is highly unusual and perhaps implies a unique chemistry. Large lenticular ultramafic bodies that are variably magnetic, are associated with both units. The lithic fragments within the mélange unit include Mather Gorge rocks, metavolcanic schists, metagabbro, and ultramafics (Drake and Lee, 1989). These formations have had a complex structural and metamorphic history. This complexity in history is reflected in the pattern of magnetic anomalies in the Maryland and Northern Virginia Piedmont.

Short-wavelength Anomalies and Diabase Intrusions

The diabase intrusions that compartmentalize subsurface flow regimes have tight spatial signatures on aeromagnetic anomaly maps. Typically, the short-wavelength intra-basin anomalies are associated with diabase lopoliths, major diabase dikes, and prominent sheet-like diabase bodies. Examples are the anomalies associated with the Herndon and Centreville diabase lopoliths illustrated in figures 3A and 3B, respectively. In these figures, they appear as great horseshoe-shaped anomalies that 'open' toward the north. Both the Herndon and Centreville bodies have a 'concave-up' geometry and are suggested to compartmentalize subsurface flow in three ways: by providing a low premeability floor to their sedimentary in-fill; by providing a low permeability 'ceiling' to the sediments beneath, thus promoting basal flow, and by providing a low permeability barrier to regional horizontal flow, thus bounding compartments that are several kilometers in scale. The 'Dulles compartment' is one such example. It measures about 15 km (N-S) and is bounded by the Herndon lopolith on the north and the Centreville lopolith on the south (Pierce and Ryan, 2003; Ryan and others, 2007a).

Regional Seismic Reflection Structure of Culpeper Basin Sediments and the Basin-Basement Contact

Two Virginia Tech seismic reflection lines (VT–1, the eastern line; and VT–2, the western line) have sampled the Culpeper basin's lithology and structure and have been combined to produce an (incomplete) overall transect that cuts much of the basin mid-section along a roughly WNW-ESE azimuth. Details of instrumentation and data processing may be found in Ryan and others, 2007a, however we summarize the results within the context of the present borehole geophysics survey. These two reflection lines have provided a structural context for understanding the variably-dipping sedimentary structures that comprise the fluid storage compartments for the Culpeper basin. The wells discussed in this report penetrate the upper strata of these deep compartments.

The two 2-D seismic reflection lines (VT–1 and VT–2) have been combined by projecting them onto a plane that is parallel to, but intermediately-positioned between them. When so projected, there is a 5 km gap between the west end of Line 1 and the east end of Line 2. This composite image is presented in figure 4, where the gap between the lines is labeled 'magma ascent and diabase emplacement interval'. The basin-center ends of both VT–1 and VT–2 were terminated due to the proximity of the vertically-oriented energy-adsorbing diabase bodies that core the basin's central axis. Within the basin, the progressive and systematic changes in the dips of sedimentary rocks is clearly evident: dips on the order of 10 degrees in the east (right side) transition to dips of as much as 32 degrees in the west (left side). The systematic east-to-west progressive increase in dip has been confirmed by direct field measurements in exposed sections. The basin-basement contact is also clearly evident, and in the west it is broadly consistent with a listric-like continuity of the basin basement reflector with the western border fault and, in the east, with gentle slopes that are compatible with an "on-lap" relationship between the basin lithologies and the surrounding and underlying Proterozoic rocks. In the Proterozoic rocks beneath the basin, bright reflectors have defined the layering within two broadly anticlinal structures, whose fold amplitudes are on the order of 1 second of two-way travel time, and whose wavelengths are roughly 8 to 10 km. These correspond to the Catoctin Formation metavolcanics in the west, and to the broad anticlinal structure centered over the 17 km marker point in the east. This eastern-most antiform structure is generally coincident with the Mather Gorge Formation visible in the aeromagnetic map of

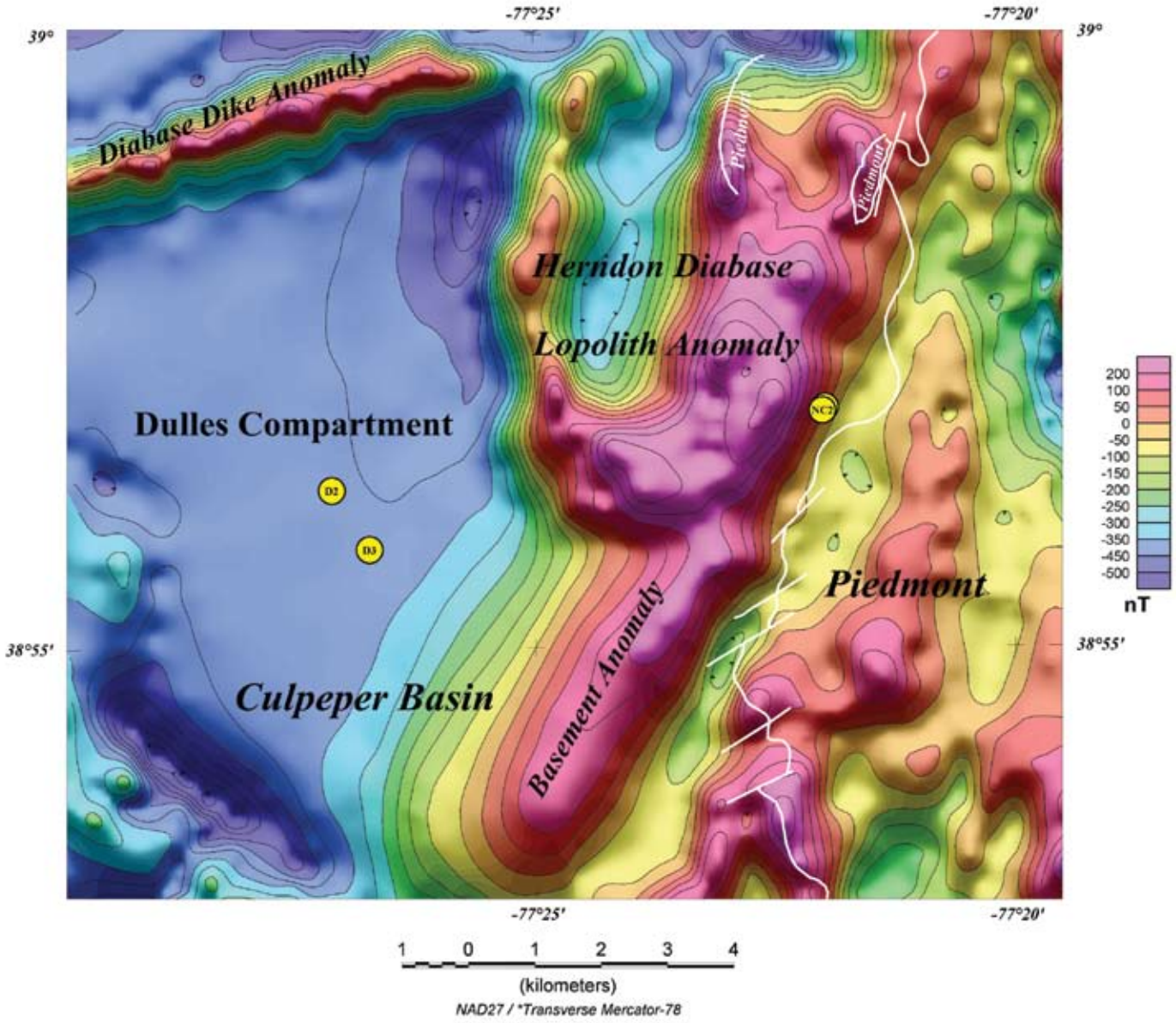

Figure 3A. Short wavelength aeromagnetic anomalies in the Herndon region of the Culpeper basin. The sinuous outline of the eastern margin of the basin is provided by the white line, including the locations of faults that pass into the basin from the neighboring Proterozoic rocks to the east. The horseshoe-shaped anomaly of the Herndon diabase lopolith (maroons and magenta) has a 1:1 coincidence with mapped locations of diabase. The anomaly itself corresponds to the upturned edges of the lopolith, and thus emphasizes it's concave-up geometry. The lopolith cradles a lens of the Poolesville Member of the Manassas Sandstone. Extending southwestward from the southern end of the lopolith is a ridge-like `basement` anomaly, a fraction of which corresponds to a narrow mapped diabase dike. In the northwest lies the ENE-WSW striking diabase dike that crops out along Rte. 606 (Old Ox Road), north of Dulles International Airport. South of that dike, lies the Dulles compartment, comprised of Balls Bluff Member siltstone (shown here in blue and purple). Borehole geophysical survey locations at the Airport are given by the pair of yellow dots.

figure 3. Indeed, the Catoctin Formation metabasalt anomaly and the Mather Gorge Formation anomaly are two of the three long-wavelength anomalies that move beneath the Culpeper basin from northeast to southwest and then to the south and southeast, as illustrated earlier in figure 3. These two structures are among three broad antiform subsurface structures that may be traced for about 400 km from Maryland to northern Georgia (Çoruh, et al., 1988). The third long-wavelength anomaly is the Sykesville Formation, east of, but parallel to the Mather Gorge Formation, as remarked above.

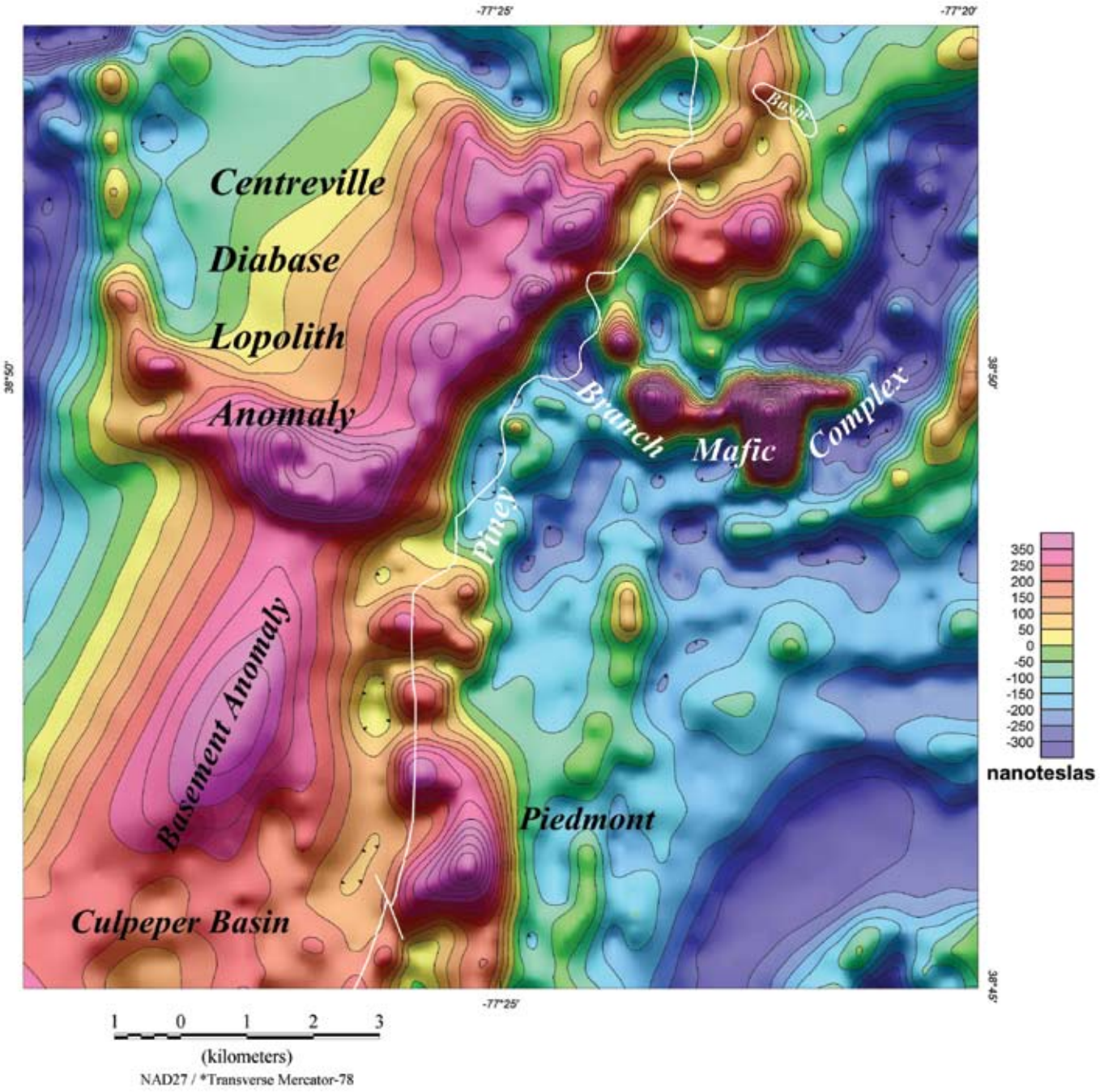

Figure *3B*.—Short wavelength aeromagnetic anomalies in the Centreville region of the Culpeper basin. The eastern basin margin is given by the sinuous white line. The Centreville diabase lopolith anomaly is the horseshoe-shaped feature that dominates the north (maroons), and cradles a lens-shaped inlier of Balls Bluff Member siltstone in its concave-up interior. The `basement anomaly` that extends to the southwest from the lopolith, is strikingly similar to its counterpart in the Herndon area (fig. 3A). The Piney Branch Complex is an anomaly within the Proterozoic crystalline rocks that lie just outside the basin.

Proposed Compartmentalization of the Culpeper Basin

Basin Compartmentalization by Intrusive Complexes: Diabase Septa and their Function.

The Culpeper basin is approximately 132 km in length and about 34 km at maximum width. The basin is cored along its central axis with a great complex of diabase dikes, sheets, lopoliths and irregularly-shaped mafic bodies. The relatively low fluid permeability of diabase is typically in the range $10^{-17} < k < 10^{-21}$ m^2, and this low permeability is broadly correlated with relatively high electrical resistivities. Permeability values

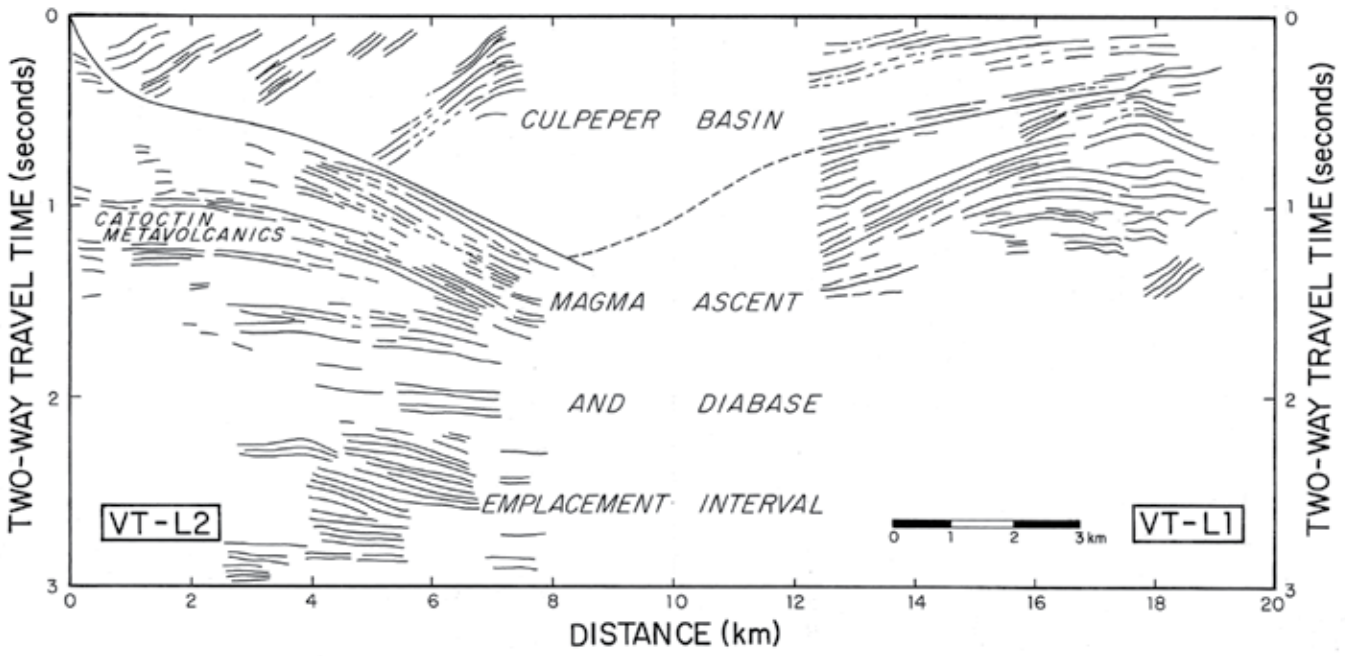

Figure 4. Synthesized synoptic structural cross-section across the Culpeper basin, based on reprocessed seismic reflection lines supervised by John Costain and Cahit Çoruh of the Virginia Tech Regional Geophysics Laboratory (after Ryan, et al., 2007a). VT–L1 and VT–L2 refer to two seismic lines that approached each other across the basin. The gentle westward dips of the sedimentary rocks on the eastern side of the basin contrast strongly with the pronounced steeply westward dipping attitude of sediments in the western portion of the basin. The sediments are massively fractured in ways that promote fluid storage and migration, and they comprise the core regions of the Culpeper basin's groundwater compartments. The seismic section is from west (left) to east (right) and spans the distance from Aldie to Fairfax, Virginia. Shallow bright reflectors denote the progressively-westward dip of intra-basin sediments, as well as the gently antiformal-configured Catoctin metavolcanics in the west and their Proterozoic basement counterparts beneath the basin in the east. The locus of diabase magma ascent and emplacement occupies the central portion of the cross-section. Two-way travel times of 3 seconds for rocks of these velocities correspond, very broadly, to about 9 km depth.

of 10^{-17} m^2 and lower are considered to be virtually impermeable (for example, Bear, 1972, 1979). The permeability of the surrounding sandstones, siltstones, and conglomerates is typically in the range $10^{-12} < k < 10^{-14}$ m^2 (with correlative lower electrical resistivities). There are therefore at least three orders of magnitude—and potentially upwards of nine orders of magnitude—difference in permeability between the diabase units and their sedimentary surroundings. This implies that bodies of diabase are expected to deflect, impede, impound, and otherwise strongly interfere with the regional flow of groundwater in the basin. Where complexly arranged in vertical stacks of sheets and/or horizontal boxworks of intrusives, these bodies are suggested to compartmentalize the basin flow—both horizontally and vertically. Predicted (but not yet tested) implications of such compartmentalization, if real, include the potential for: (a) somewhat stagnant flow at depth within a compartment, and relatively freely-flowing fluids at shallow levels; (b) isotopically old groundwater deep within a compartment, and progressively younger waters at shallow levels; and (c) higher amounts of total dissolved solids in compartmentalized waters, and lower values in the near-surface. One can thus think of the Culpeper basin as a great 'super-tanker', where the diabase bodies act as bulkheads within this conceptual vessel. Ryan and Yang (1999), and Ryan and others (1997, 2000, 2002, 2007d) discuss compartmentalization in low and high temperature systems, including the roles of fractures on hydrothermal convection, and Laczniak and Zenone (1985) outline the roles of pumping test scenarios on the hydrology of sections of the Culpeper basin. Ryan et al., 2007a, 2007b, and 2007c illustrate how diabase bodies deflect, impound and compartmentalize local and regional flow. These authors also show how diabase bodies comprise groundwater divides—systematically complicating the regional flow patterns with the superposition of local topographic influences.

A Concise Summary of Relationships Suggesting Basin Compartmentalization

Several lines of evidence suggest that the Culpeper basin is hydrodynamically compartmentalized today and was similarly compartmentalized during the Mesozoic when Lower Jurassic intrusions and eruptions completed the three-dimensional internal structure of the paleo-basin and excited hydro-

thermal convection. The evidence for compartmentalization is presented and discussed in Ryan and others, (2007a, 2007b and 2007c), and in Pierce and Ryan, (2003), and includes:

1. The relatively low permeability of diabase relative to surrounding hornfels and sandstone/siltstone sequences.

2. The typically relatively low pumped groundwater yields from wells sited within diabase vis-à-vis wells sited within neighboring sandstones or siltstones.

3. The ubiquitous nature of diabase within the basin, its wide three-dimensional distribution and volumetric signficance.

4. Frequently (but not universally) observed high values for groundwater heads measured in wells on the recharge side of diabase bodies vis-à-vis measurements collected on the discharge side.

5. Contact springs (single and multiple) located on the recharge side of diabase bodies and the evident absence of systematic contact spring development on the discharge side.

6. Abnormalities in the pumped drawdown curves for wells proximal to diabase contacts consistent with the perturbation of the developing cone of depression by a no-flow or low-flow boundary coincident with (i.e., identical to) the diabase body.

7. Order of magnitude differences in the electrical conductivity of diabase and neighboring sandstone/siltstone sequences as revealed by magnetotelluric (MT) and audiomagnetotelluric (AMT) measurements. Diabase resistivities are typically ~1,000 to ~4,000 ohm-m, whereas sandstone/siltstone resistivities range over ~60 to ~400 ohm-m.

8. Analytic (complex variable-based) treatments of flow processes adjacent to impermeable boundaries illustrate the profound roles of diabase in deflecting and impounding groundwater.

9. Finite element simulations of the effects of diabase intrusives on subsurface flow in model basin volumes as functions of progressive contrasts in permeability between the diabase and surrounding sandstones and siltstones. Such studies have constrained the permeability contrasts required between diabase bodies and their surroundings for the onset of compartmentalization.

We (Ryan and others, 2007b) have also evaluated the geometry of diabase bodies in the Gettysburg and Hartford-Deerfield basins in relationship to to their potential roles as compartment boundaries, and find consistency with the relationships discovered within the Culpeper basin. By extension then, these relationships suggest also that the Gettysburg, Hartford, Deerfield—and likely the Newark ~~-ba~~sins are similarly compartmentalized although the details of this compartmentalization may differ.

Throughout this report, references will be made to the Dulles compartment, the Gainesville compartment, and the Rapidan compartment, among others. These names are used informally, and when the term "compartmentalization" is used, it is understood that it should be read "proposed compartmentalization".

Scientific Objectives and Borehole Field Experiment Strategy

Our borehole geophysical and geological logging program was initiated in 2000, and is part of a broader program of geophysical and geological research aimed at understanding the contemporary—and paleo-fracture flow hydrology of the major Mesozoic basins of eastern North America. We seek to understand the three-dimensional structure of the Culpeper basin and the geometric interrelations between primary basin rock types and their bearing on subsurface flow. Of particular interest are permeable rocks that store significant volumes of groundwater, which are transmissive, and that therefore comprise important aquifers. Fracture flow and fracture-based storativity is of particular interest in this context. Examples of such high storage capacity rocks are the Balls Bluff Member of the Bull Run Formation and the Poolesville Member of the Manassas Sandstone within the Culpeper basin of Virginia and Maryland (see the geologic reference maps of figures 5A and 5B). However equally important hydrodynamically are the relatively impermeable rocks since, if widely and systemmatically arranged within the basin, impermeable rocks have the potential of acting as internal 'no-flow' boundaries, thus contoling the rate, direction and extent of fluid migration, as well as several aspects of the basin's internal groundwater storage. The prime example of such impermeable rocks are the massive diabase bodies that occur throughout the Culpeper basin (Ryan and others, 2007a, 2007b).

Our experiments have been designed to determine aspects of the lithologic, structural and hydrologic properties of several Culpeper basin rock types. Parameters of interest include the formation electrical resistivity structure, bedding plane fractures, cross-bedding fractures, electrical conductivity of the borehole fluids, the temperature-depth distribution in the well bore fluid, the first derivative of the temperature-depth distribution ($\frac{DT}{DZ}$), and mineral lineations and small-scale lithologic variations from millimeter-to-meter scale range. Lithologic variations of interest include the relative clay contents, mineral layering, and vein distributions and their geometry. We would like to relate these lithologic and structural variations to the broad structure of the groundwater compartment within which it is found, or alternately, to the transition from the compartment-bounding diabase intrusion to the adjacent hornfels. Where possible, we also wish to relate the inferred

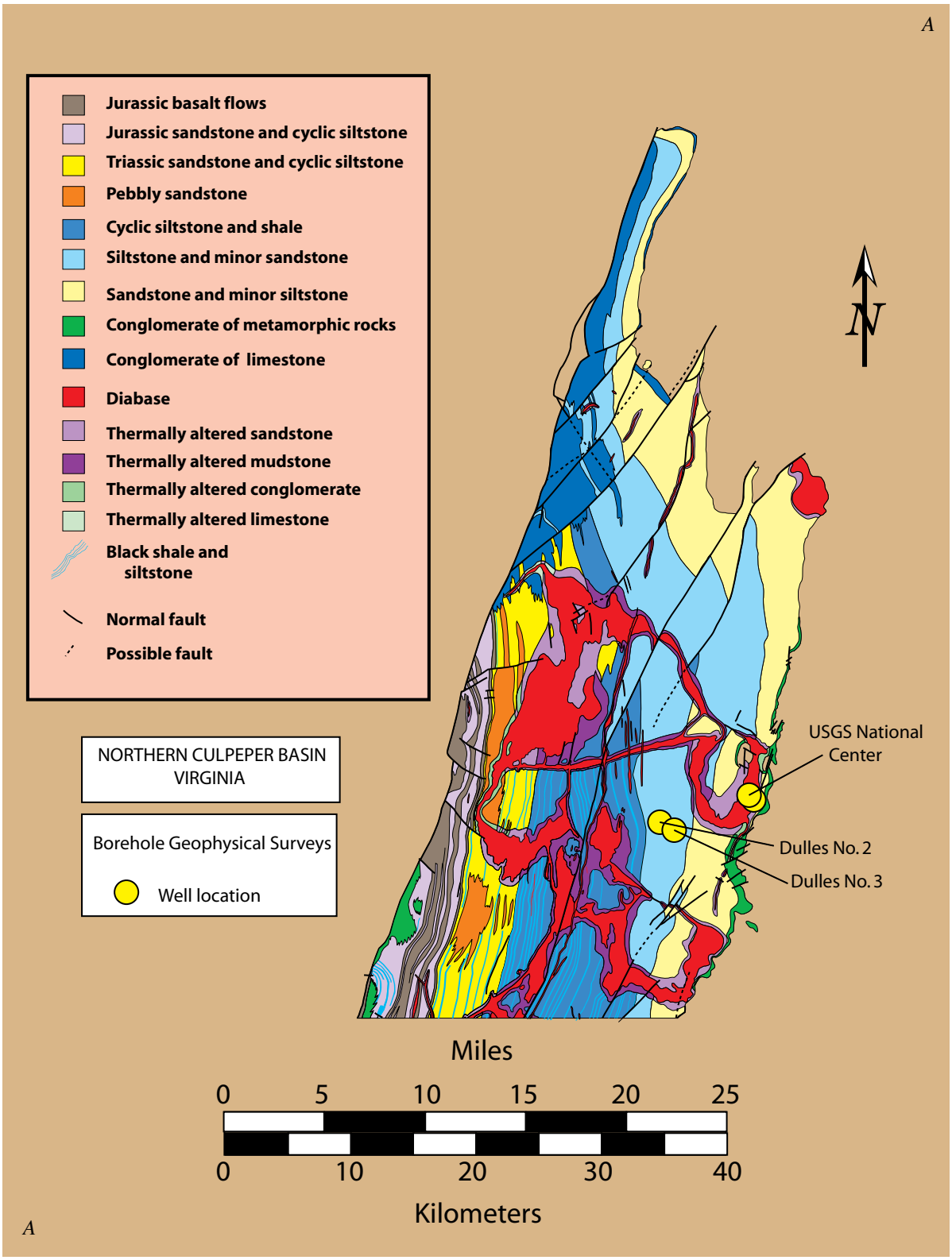

Figures 5*A* and 5*B*. Borehole geophysical survey locations within the northern (A)and southern (*B*) Culpeper basin superposed on principal geologic units. Principal diabase lopoliths, dikes and sheets are denoted in red, and their thermal metamorphic haloes are given in dark pink (surrounding red diabase). The primary sites are, from north to south, Dulles International Airport; U.S. Geological Survey National Center campus in Reston, Virginia; Gainesville, Virginia; and Rapidan, Virginia. Color coding on lithologic units is: light yellow (Poolesville Member of the Manassas Sandstone); Light blue (Balls Bluff Member of the Bull Run Formation);

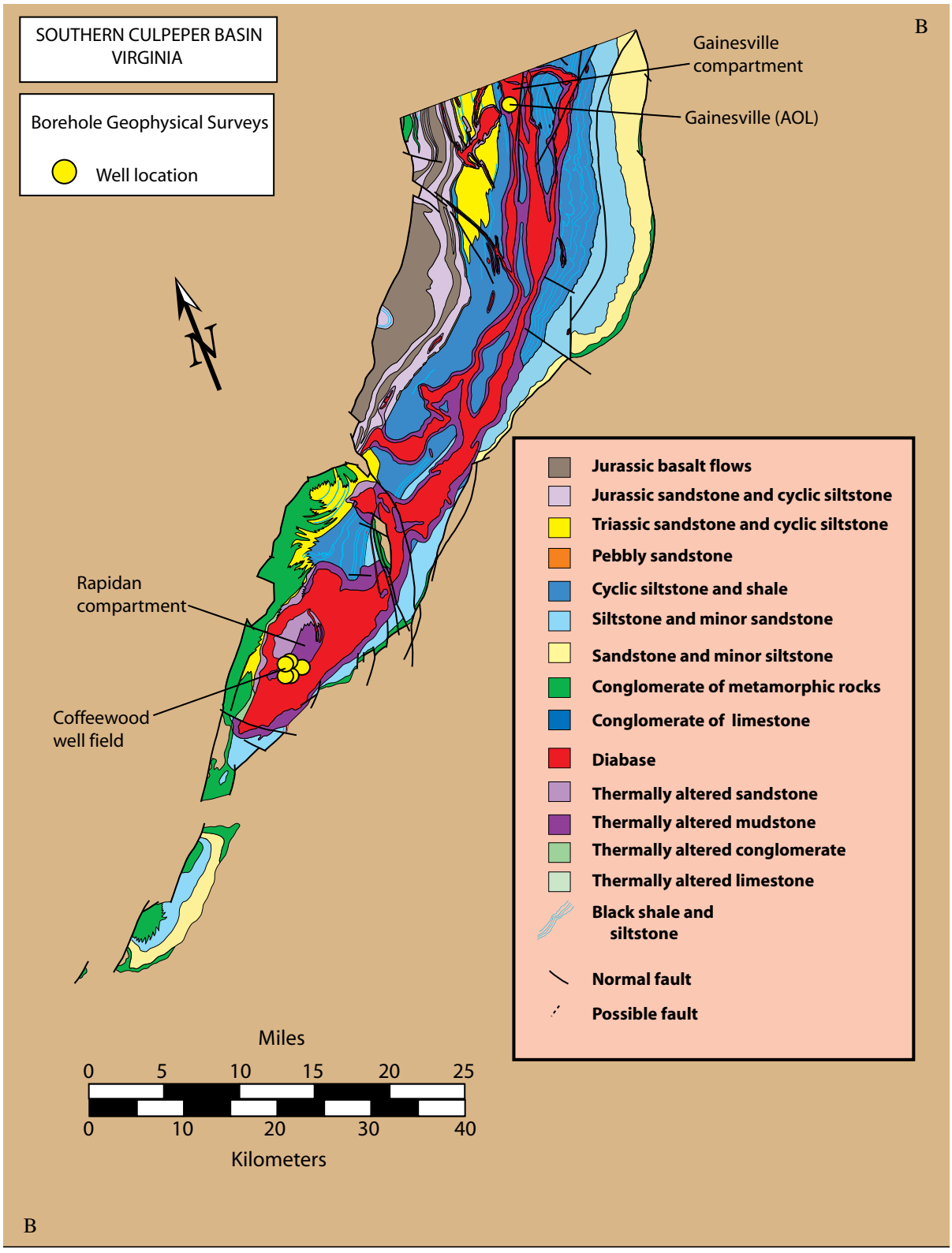

5A and 5B. (Continued) Medium blue with light blue striations (alternating lacustrine and fluvial phases, of the Balls Bluff Member); Medium green (Turkey Run Formation); bright yellow (Catharpin Creek member); Orange (Goose Creek Member of the Catharpin Creek Formation (a conglomerate)); Light pale Blue in western portion of basin (Midland Formation); Brown (Sander Basalt); Brown (Hickory Grove Basalt); and Bright green (Cedar Mountain Member of the Bull Run Formation (a "border" conglomerate)). Proposed compartment names are indicated with leaders to their respective locations.

lithologic and structural variations seen in boreholes with their counterparts seen in outcrop exposures. Borehole geophysics and geology are critically important for guiding the continuing development of conceptual models of fracture flow, and in ultimately properly constraining derivative numerical models of subsurface fluid migration.

Four study areas within the Culpeper basin have been selected for reconnaissance borehole logging. These include locations within the proposed Dulles compartment, the Gainesville compartment, the Rapidan compartment, and the U.S. Geological Survey's National Center campus (figs. 5A and 5B). Each location explores different aspects of the geologic environment of fluid storage and migration. Within the Dulles compartment, we have used deep wells at Dulles International Airport to sample the structure of the Balls Bluff Member of the Bull Run Formation the dominant aquifer and rock type at this location, and throughout much of the central portion of the basin. Within the Gainesville compartment, we have used a relatively deep well that penetrated the compartment-sealing diabase lopolith and penetrated the subjacent permeable hornfels, to explore the physical nature of compartment septa, or "bulkheads", and the establishment of basal flow regimes. At the Rapidan compartment, we have logged an array of wells that have been sited within the hornfels lens of metamorphosed Balls Bluff Member siltstone, cradled within the concave-up interior of the Rapidan lopolith. And at the U.S. Geological Survey's National Center, we have used two monitoring and test wells to examine the nature of the Culpeper basin`s eastern structural margin, where Mesozoic basin rocks have an on-lap relationship lying unconformably on the adjacent Proterozoic rocks. Each of these environments with selected results from reconnaissance logging are discussed below.

The Proposed Dulles Compartment

Dulles International Airport rests on top of a large proposed subsurface groundwater compartment (see figs. 2, 3A and fig. 5A). The proposed compartment is bounded on the north by a prominent diabase dike exposed along Virginia route 606 (Old Ox Road) in the vicinity of the Dulles Greenway, bounded on the south by the Centreville diabase lopolith, and bounded on the west by the irregular diabase body beneath the western margins of Dulles Airport property, in combination with a swarm of N-S-alligned diabase dikes. It is also largely bounded to the east by the western margins of the Herndon diabase lopolith. Contained within, is a large expanse of Balls Bluff Member siltstone and thermally-metamorphosed remnants near the diabase contacts. The inferred systematic closure of the Balls Bluff Member fractures with depth (due to progressive increases in the horizontal components of confining pressure) is inferred to effectively 'floor' the compartment, by analogy with experimental results on other—yet roughly similar—lithologies (Ryan, 1987). The fluids within the compartment are thought, strictly however, to be partially compartmentalized, since just east of the airport a small subsurface opening near the Herndon lopolith occurs. We refer to this portion of the Culpeper basin as the "Dulles compartment". The electrical resistivity structure of the Dulles compartment, as well as other compartments within the Culpeper basin have been studied by AudioMagnetotelluric [AMT] surveys, and is presented in the companion report of Pierce and Ryan (2003).

Balls Bluff Member of the Bull Run Formation

Both lacustrine and fluvial phases of the Balls Bluff Member siltstone are exposed in the Culpeper basin (Lee and Froelich, 1989; Smoot, 1989, 1991; Faill, 2003, and J.P. Smoot, unpublished mapping). The sequence astride the Dulles airport access road (just west of VA Rte. 28), for example, contains thin beds colored a deep rust orange and having distinctive westward dips. Inferred paleo-dessication of the uppermost portions of beds occassionally has produced dehydration shrinkage fractures arranged in crudely polygonal patterns that extend vertically downward into the rock mass from bedding planes. The mineralization (calcite and quartz-dominated) within these polygonal networks are thus remnants of some of the first 'fracture flow events' during basin evolution. Within a bed, an upward decrease in clay content and an increased volume fraction of sand may be consistent with correspondingly higher permeability, the development of matrix flow, and for subsequent epidote mineralization during thermal metamorphism, a common association in field exposures (Ryan and others, 2007a).

Fracture patterns in the Balls Bluff Member include bedding plane fractures and cross-bedding fractures. Both the bedding plane and cross-bedding fractures are consistent with origins dominantly related to decompression-induced expansion during erosional unroofing. Mineralized fractures corresponding to paleo flow events are typically open today, and available for contemporary groundwater flow. Cross-bedding fractures tend to be mutually orthogonal to each other and they are also collectively orthogonal to the bounding bedding planes. This overall fracture geometry produces an orthorhombic fracture network in three dimensions, when the Balls Bluff Member is considered as a whole. Thus the Balls Bluff fracture systems define a crudely "brick work" geometry in three-dimensions. This "brick work" or crudely orthorhombic geometry is suggested to be a recurring theme in the fracture-controlled permeability at shallow depths within much of the basin. Contemporary apertures of 0.1 mm correspond to approximate permeabilities of 8. x 10^{-10} m^2 [800 darcys], whereas apertures of 4.0 mm correlate with approximate permeabilities of 5. × 10^{-6} m^2 [mega Darcy range]. Within the Balls Bluff Member fractures, zeolite facies metamorphism (proximal to adjacent diabase heat sources) have crystallized calcite, $CaCO_3$; stellerite, $Ca(Al_2Si_7O_{18})7[H_2O]$; gedrite, $(Mg,Fe^{+2})_5Al_2[Si_6Al_2O_{22}](OH,F)_2$; and chabazite, $CaAl_2Si_4O_{12}$ $6[H_2O]$ identified in hand samples. The thickness range for the Balls Bluff is from about

80 m near the northern margins of basin, to about 1,690 m in the central portion of the basin. The distribution of the Balls Bluff Member may be seen in figures 5A and 5B.

Geophysical Logging in the Proposed Dulles Compartment

The lithology of the Dulles compartment as determined by borehole logging is almost entirely Balls Bluff Member of the Bull Run Formation. However outcrop inspection on the western portions of Airport property indicate the presence of minor hornfels (after Balls Bluff Member) due to thermal metamorphism above a diabase sheet heat source. This diabase sheet is actively being quarried to the east-southeast of the US Route 50 and VA route 606 intersection. The quarry operator is the Chantilly Crushed Stone Corporation. The Dulles compartment depth is not known in detail, however 2-D seismic reflection profiling (Ryan and others, 2007a) is able to roughly estimate the depth at about 1.5 to 2.0 km.

Preliminary logging on Dulles International Airport property was conducted in 2001. Two wells were logged. Well No. 2 was logged to a depth of 289 m (original depth of the well was 290 m), and well No. 3 was logged to 43 meters (the original drilled depth was 290 m; thus the lower 247 m has been silted-in or bridged since well completion). Both wells were logged for the fluid temperature-depth function and the first derivative of temperature with depth or 'delta temperature' ($\frac{DT}{DZ}$), formation electrical conductivity and resistivity, fluid conductivity and resistivity, natural gamma, and caliper data (see figs. 6 and 7). Further characterization of the proposed Dulles compartment would benefit from optical and acoustic televiewer logging, heat pulse flowmeter logging and electromagnetic (E-M) flowmeter logging. Based on the total depth estimates for the Dulles compartment as discussed above, the maximum well penetration from work conducted thus far is suggested to be about about 14 to 16 percent of the overall compartment depth as estimated by seismic reflection.

The WellCAD borehole geophysical logs for Dulles wells No. 2 and 3 are organized in a five column format (see figure 6): column 1 contains the three-arm caliper, casing and lithologic information based on cuttings; column 2 contains the formation resistivity (Ohm-m) and conductivity (mmho-m) data; column 3 contains the fluid temperature (°C and °F) and temperature derivative as a function of depth (dimensionless) data; column 4 presents the fluid resistivity (Ohm-m) and fluid conductivity or specific conductance (micro-Seimens/cm); and column 5 presents the natural gamma counts (counts per second) as a function of depth.

The entire section within wells No. 2 and 3 is within the Balls Bluff Member, and the wells are far removed from the lateral diabase boundaries that define the margins of the Dulles compartment. Thus the purpose of the Dulles logging is the characterization of the Balls Bluff Member well within a compartment interior. Subtle variations with depth in the temperature of the ambient water column may contain information relating to localized water inflow or outflow from the borehole. In the absence of flow, the borehole temperature reflects the geothermal gradient, where a rough rule of thumb indicates an increase in temperature of about 1 degree per 100 ft of depth. Active flow into or out of the borehole, however, has the potential to perturb the linearity in the T-Z profile. An indication of differential seepage from fractures is a spike in the temperature derivative, $\frac{DT}{DZ}$, suggesting a local inflection in the T-Z profile. Within the Balls Bluff Member, at least 33 such spikes in the temperature derivative occur in Dulles well No.2, suggesting the possible influx of water along fractures at these levels. The T-derivative spikes are unevenly distributed with depth, however field observations of the Balls Bluff Member in outcrop, suggest that bedding plane fractures are a prime contributor to bulk fracture flow.

The Proposed Gainesville Compartment

Direct Drilling into the Gainesville Compartment

An additional confirmation of the validity of the compartmentalization model was demonstrated during well drilling in July of 2001, at the America On-Line (AOL) data storage facility at Gainesville, Virginia. Drilling was performed by Mark McClellan and Duane Sturgill of Groundwater Systems, Inc., under contract from HIS-GeoTrans of Sterling, Virginia, and the Poole and Kent Corporation of Baltimore, Maryland. The AOL facility was sited on the Gainesville diabase sheet, just south of the intersections of routes US Interstate 66 and Virginia Route 29 (see site location in figs. 5A, B). The very low permeability of the diabase yielded correspondingly low flow rates: about 2 gal./min. Five holes drilled into the diabase sheet continued to produce negligible (low flow rate) results. The last hole, however, was drilled into and just through the diabase sheet, to a depth of about 225.5 meters (740 ft.), and completed or terminated in the highly fractured and permeable hornfels of the compartment's margins. The flow rate (within the hornfels) was about 100 to 110 gal./min. (Cohen, 2001)-sufficient for AOL to use as cooling water for their data storage center. The overall flow rate for the entire well—incorporating the low productivity of the diabase—was 90 gpm based on air-lift testing conducted by Groundwater Systems, Incorporated.

Flow testing based on pumping at 100-110 gpm has been used to develop time-drawdown curves for the production well and evaluate the transmissivity (T), storage coefficient (S), and leakance parameter (B), using the Theis equation and the Hantush leaky aquifer solution (Cohen, 2001). These tests characterize the relatively fractured and thermally- metamorphosed Balls Bluff Member of the Bull Run Formation (hornfels) in the transition region between the hornfels and the overlying

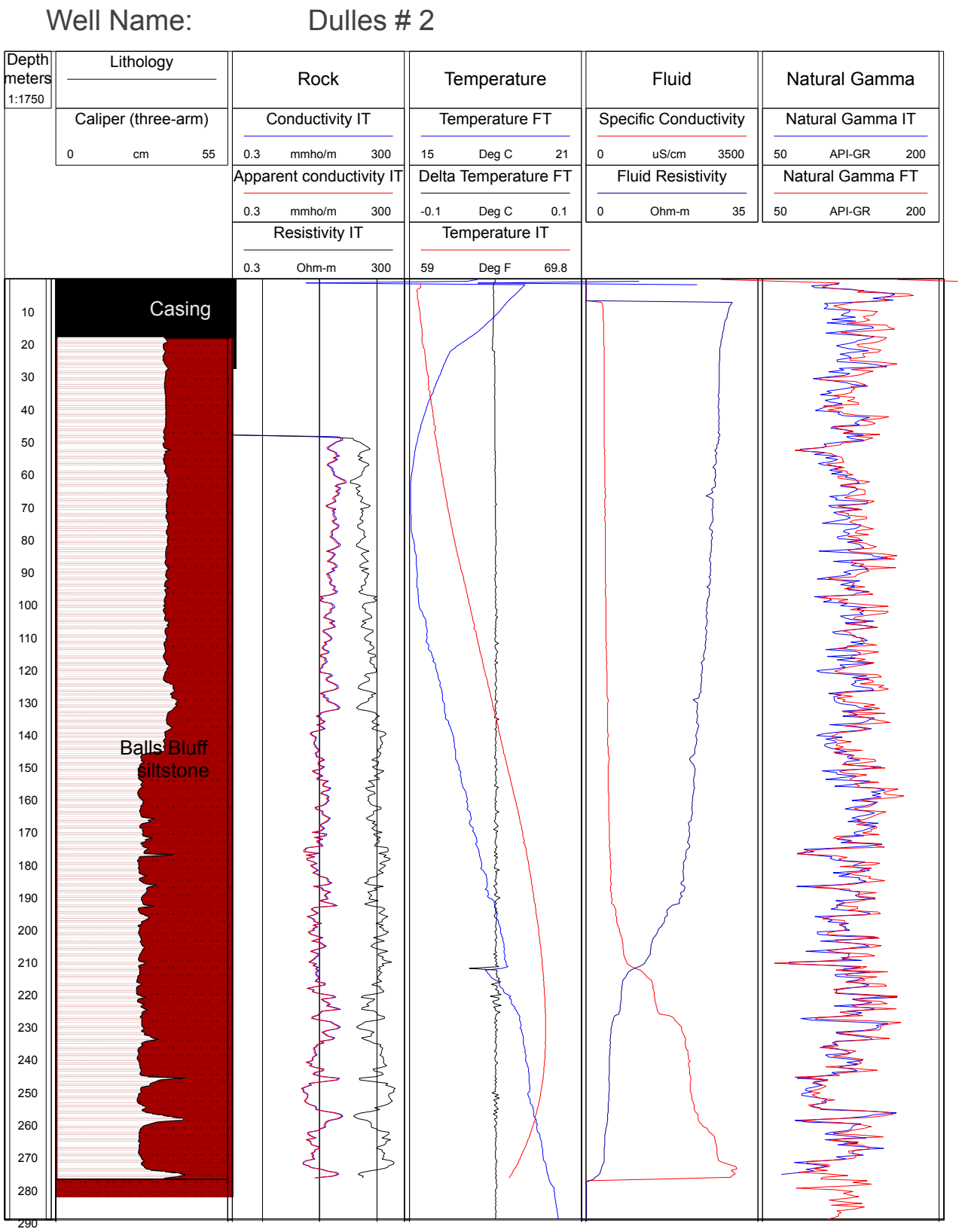

Figure 6. Geophysical logs from Dulles well No. 2 at the Washington Dulles International Airport.

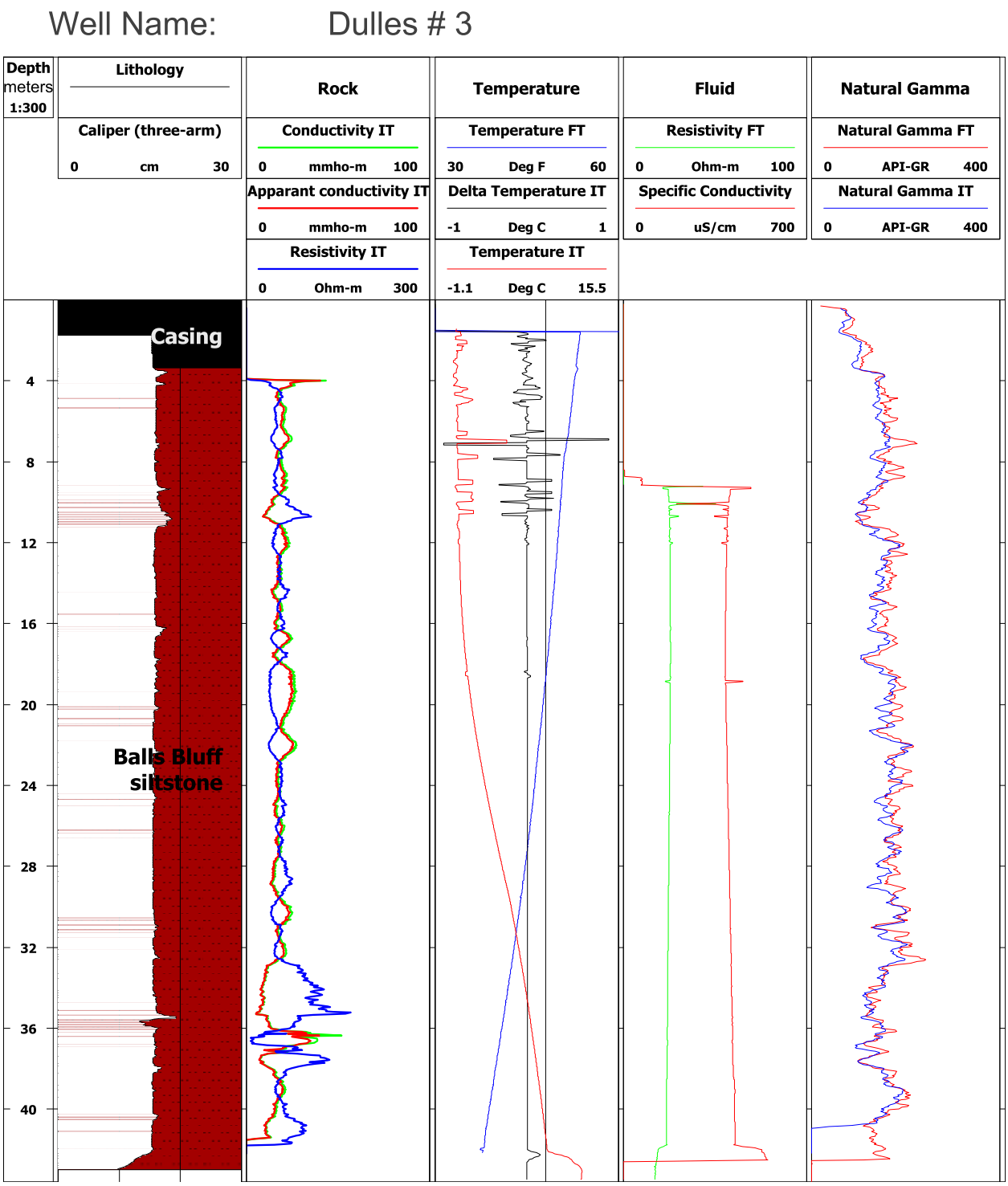

Figure 7 Geophysical logs from Dulles well No. 3 at the Washington Dulles International Airport.

diabase. For the Theis simulations, transmissivities and storativities were 2.909 x 10^{-2} ft^2/min and 5.145 x 10^{-2}, respectively, whereas for the Hantush leaky aquifer simulations, the transmissivities were 1.902x10^{-2} ft^2/min., with a storativity of 1.267x10^{-1}, and a leakance parameter of 2.889x10^{-2}.

Geophysical and Geological Logging Through the Proposed Gainesville Compartment Margins and into the Compartment Interior

The WellCAD logging data for the Gainesville borehole is organized into four primary columns (fig. 8): Column 1 contains the optical televiewer (OTV) data. The orientation scheme begins with the N-E-S-W-N sequence from the left hand margin, through a sequence of ruled vertical lines, to the right hand margin. Thus the viewer moves progressively clockwise around the borehole's inside circumference in looking at the data from left-to-right on the plot. These cardinal directions correspond, in turn, to the compass azimuth directions familiar to field geologists: 90, 180, 270, and 360 degrees, respectively. The OTV data have been analyzed with WellCAD (4.2) software and several picks of geologic features have been made. The features have the following color codes: black: fractures showing no relative lateral displacement (joints); dark blue: fractures showing some lateral displacement (faults); light blue: mineral veins; green: bedding-conformable mineral layering; pink: highly-inclined to near-vertical fractures. Mineral layering within the diabase tends to be pyroxene-rich, whereas mineral layering within the hornfels tends to be clay-rich. Column 2 contains the virtual core. This image is highly pixelated and serves schematic purposes only. The 'ledges' of the core may correspond to the locations of fractures. Column 3 contains the three-arm caliper plot and the inferred lithologic log. Finally, column 4 contains the temperature-depth plot.

Within the full and extended version of WellCAD (4.2) or the free WellCad reader (4.2) the virtual core may be manipulated to reveal or enhance lithologic and/or structural features. These manipulations include core rotation, axial core compression, axial core extension, slicing, or along-axis "halving", and multiple (split screen) presentations of several cores simultaneously. A "northside marker" along the core axis denotes the 0-degree position, which is magnetic north. This marker will appear as a thin colored line along the core length.

The 'unwrapped' core reveals the same structures that the virtual core depicts, and usually at much higher resolution, due to the pixilation requirements of quality virtual core construction. In extended WellCAD (4.2), the unwrapped presentation may be compressed or extended as desired, and changes in the resolution and visability of features will progressively change in the process. Such changes in scaling may be done without "loosing" the top or bottom of the core. Core compression has the advantage of concise summary presentations of data for, for eample, side-by-side comparisons with core sections from neighboring wells or boreholes. For maximum detail and resolution, however, scale extension is recommended. Extension may continue to be applied until image degradation is noticed. Settings may then be "backed off" until resolution is maximized.

Planar features such as brittle elastic fractures, faults, veins, and mineral layering, are seen as horizontal lines or bands in the core sections if they have no significant dip. The same features will appear as sinusoidal lines or sinusoidal bands of various amplitudes and wavelengths if they dip. The larger the dip, the larger their amplitude on the unwrapped core section. Sinusoidal features with particularly high amplitudes are, therefore, high-angle or steeply-dipping features. Examples of such features may be seen in figures 8A and 8B.

Once "unrolled" and extended so that lithologic and structural features can be seen with clarity, specific "picks" can be made using the full and extended WellCAD (4.2) software. In the core sections provided in this report, picks of fractures, veins, mineral lineations, and faults have been made only where there was clear indication that the feature was complete and untruncated by other structures/lithologies. Thus, only a fraction of the total population of these features has been selected for viewing.

The geology sampled in this borehole consists of a part of the Gainesville diabase sheet within the upper 183 m, and hornfels (after the Balls Bluff Member) in the lower 43 m. The diabase is heavily fractured, and the picks provided show a tendency for the fractures to be either slightly dipping (to the ENE over the 50-160 m interval) or to be relatively flat-lying (the 152-200 m interval). The origin of the subvertical fractures in the diabase may be ascribed to both a thermal and a tectonic (regional stretch) component. In the OTV images, near-vertical fractures are rare (a sampling artifact of the vertical orientation of the borehole) whereas sub-horizontal fractures are plentiful. Ryan and others, (2007a) suggest that such horizontal fractures in diabase are subordinate to subvertical fractures, are the products of erosional decompression, and that they die out rapidly with increasing depth. This view is based on the prevailing occurrence of abundant subvertical fractures in diabase outcrops, and the distinctly subordinate numbers of subhorizontal fractures. Furthermore, and based in part on examination of three-dimensional outcrop exposures in combination with the borehole data, the fractures resolved in this OTV image seem to be relatively poorly-interconnected both laterally and in three-dimensions, since the pumped flow rates from the upper 183 m were less than 2 g.p.m. as inferred from air lift testing. In actively worked diabase quarries within the Culpeper basin, the sub-horizontal fractures die out rapidly with depth, leaving only the numerically-dominant vertically-oriented fractures exposed. It is important to realize, therefore, that a reliance on only borehole OTV data causes a distinctly misleading picture of the nature of the diabase fracture populations.

As may be seen in both the three-arm caliper plot as well as in the virtual core, the hornfels is highly fractured. This relative intensity of fracturing marks one of the principal indicators for identifying the diabase-to-hornfels transition

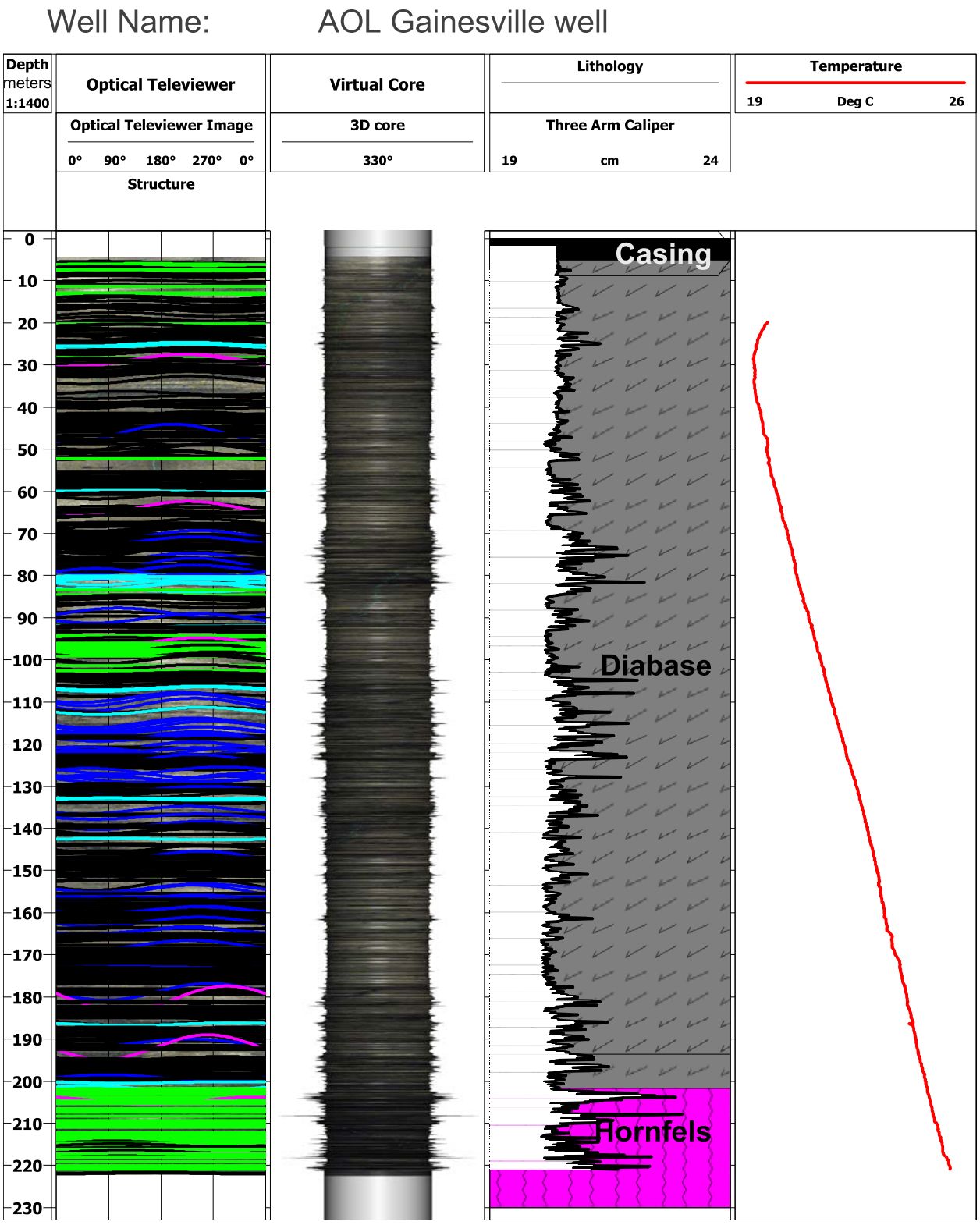

Figure 8. The America On-Line (AOL) Gainesville, Virginia well showing diabase in the upper portion of the well and hornfels in the lowest portion. This image is included in the attachments as a WellCAD WCF type file for the WellCAD reader

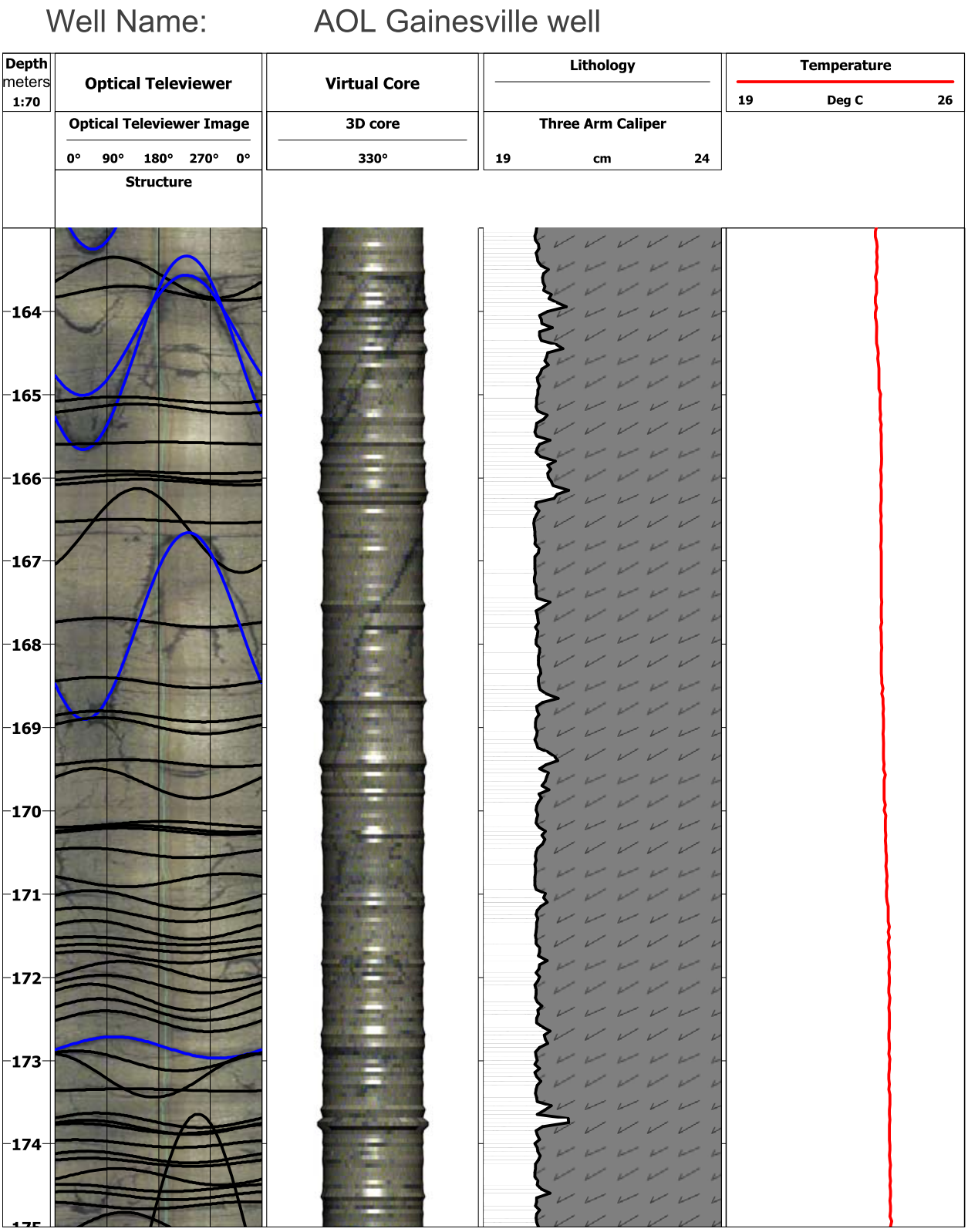

Figure 8A. WellCAD image of the 164 to 174 m interval in the AOL well at Gainesville, Virginia through the Gainesville diabase sheet. The image illustrates the running caliper record (third column with gray background and checked pattern), the virtual core (3-D image) and the unwrapped borehole wall with several fracture 'picks' shown as black and blue lines with sinusoidal geometry where fractures are steeply dipping, and gently 'rolling' geometry where fractures have negligible dips. (Left column).

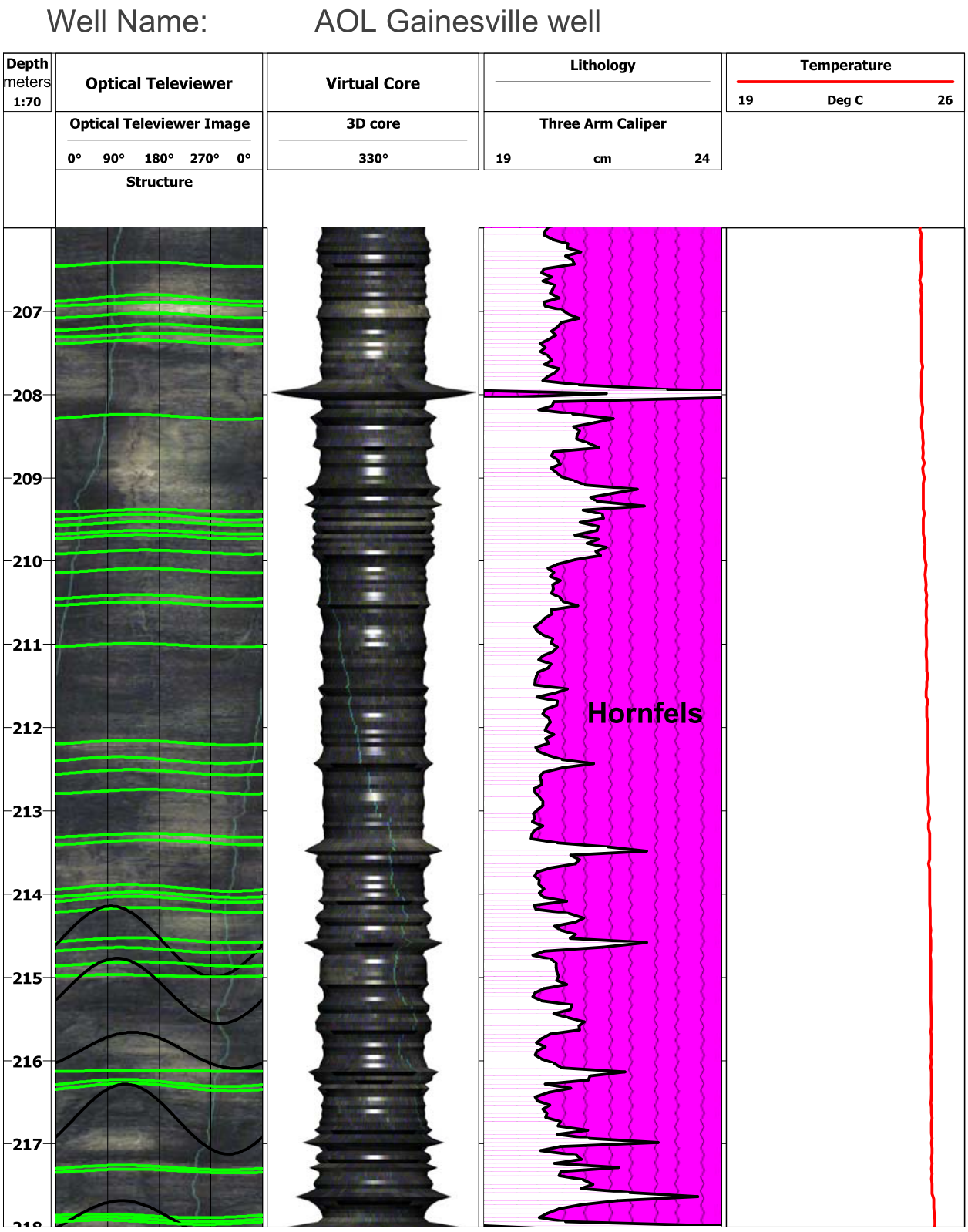

Figure 8B. WellCAD image of the 207 to 217m depth interval for the America On-Line well through the Gainesville diabase sheet. The image shows hornfels immediately beneath the diabase, where fine green lines on the optical televiewer log represent mineral lineations produced by thermal metamorphism (after clay varves in the parent Balls Bluff Member siltstone). From left to right on the figure: Metric depth scale; Unwrapped borehole walls of the optical televiewer, illustrating the hornfels fabric with mineral lineations; Virtual core (note the high amplitude breakouts correlating with fracture intersections, especially near the top at 208 m depth); Caliper record (crenulated line with red-pink pattern).

zone. Others include an abrupt increase in the number of clay-rich relect mineral lineations (the green WellCAD picks in the OTV log). The massively-fractured nature of the hornfels below the diabase-hornfels contact coupled with an inferred increase in 3-D fracture interconnectivity is linked with the abrupt jump in pumped flow rates (from less than 2 g.p.m. in diabase to about 110 g.p.m. in the adjacent hornfels). The abrupt deflection to lower temperatures in the temperature-depth (T–Z) curve at the 186 m level, also suggests a possible additional groundwater influx. Although this fracture is in diabase, it is so close to the diabase-hornfels contact that inter-fracture communication with the hornfels may have been established. Heat pulse and E–M flow meter measurements have not yet been made within this diabase-hornfels sequence. In addition, a natural gamma log would be expected to show total gamma counts climbing abruptly from near-zero values beneath the diabase-hornfels contact—another indication that the transition interval had been reached.

Structure of the Proposed Gainesville Compartment

The results of this study suggest that the geometry of compartmentalization is more complex than the simple concept of assemblages of side-by-side vertically-oriented diabase septa (e.g.: dikes), containing large volumes of highly fractured sediments between them. In addition to that type of organization, compartimentalization operates vertically as well as horizontally. Thus, the Gainesville compartment lies, in part, beneath the Gainesville diabase sheet. Hydrodynamically, this comprises a basal flow regime, where flow is confined by the diabase sheet above (see, also, Ryan and others, 2007a). It is reasonable to suspect that other sheets and lopoliths have subjacent fluid-rich compartments as well. Such compartment interiors would be expected to be comprised of relatively heavily fractured hornfels in their immediate vicinity, grading downwards into non-metamorphosed but pervasively fractured sediments, with increasing depth. The Boyds, Belmont, Herndon, Centreville, Bealeton and Rapidan diabase bodies are all candidates for this type of compartment organization.

Fractures within the diabase are invariably mineralized, and vein systems analogous to those in the dike near Dulles International Airport (on Virginia Route 606) are well developed. Chlorite-mineralized veins and fracture walls are commonly dilatant, and may provide very local migration paths for water within the diabase. Polar plots of chlorite vein orientations show two preferred trends that intersect at high angles, and thus have the potential for 3-D interconnections within the rock mass. Similarly, polar plots of contemporary fluid flow fractures (from direct visual evidence of active zones of seepage) also have two preferred trends, and their 3-D interconnections of these fractures may promote this flow. The position of the Gainesville compartment may be seen in figures 5A, B.

The Proposed Rapidan Compartment: Deep Structure of the Rapidan Diabase Lopolith

A large intrusive body, here informally referred to as the "Rapidan diabase lopolith", is named for the largest nearby community. It has been mapped as a great sheet-like body (Lee and Froelich, 1989; J.P. Smoot and D.M. Sutphin, imformal communications, 2002). The body is a concave-up intrusive that cradles in it's interior a massive inlier of Balls Bluff Member siltstone. It rests in turn on the contact-metamorphosed-equivalent hornfels. The true geometry of the body is thus lopolithic (see fig. 5B). The results of the AudioMagnetotelluric study of Pierce and Ryan (2003) suggest that at depth the diabase body appears to be structurally weakly divided into two high resistivity lobes, however this inference rests on the data of one vertical audioMagnetotelluric (AMT) sounding station profile. We interpret this apparent division, if real, as being mainly induced by undulations in the contact zone topography between the diabase and the Balls Bluff Member at the time of intrusion. Undulations in contact topography are relatively common for mafic intrusions invading sediments, particularly if the sediments are not fully lithified, as is appropriate for the Culpeper basin. Typical examples are found in basalts as they invade soft sediments, and the Gulf of California spreading center near the Salton Sea geothermal region of California, is one such example, among other locations world-wide. In the AMT-based electrical resistivity cross-sections of Pierce and Ryan (2003), lobes of resistive diabase make contact with the mantling hornfels. These irregularities (high amplitude undulations) occur within the contact region between the diabase intrusion and the Balls Bluff Member, and are believed to have developed during intrusion. Multiple (pulse-like) intrusion episodes also produce this type of complex contact structure, and routinely incorporate lenses or screens of country rock between them. Multiple intrusion episodes are now known to have occured in both the Gettysburg basin (Ryan and others, 2007b) and Culpeper basin (Ryan and others, 2007a), and would be expected for other Mesozoic basins invaded by diabase during the Lower Jurassic. Both multiple intrusion pulses and upper contact surface undulations in intrusion-host rock topography are to be expected for the Rapidan lopolith as well as other Culpeper basin lopoliths. Screens of Balls Bluff Member siltstone caught up between diabase intrusion pulses would therefore remain today as hornfels screens, which are characteristically more intensely fractured, more susceptible to weathering, and much lower in bulk electrical resistivity than their diabase neighbors. Overall, the Rapidan diabase lopolith has a thickness of at least ~550 meters in the vicinity of Michells, Virginia, based on the AMT study of Pierce and Ryan (2003). The body is believed not to be monolithic and planar, but to have significant three-dimensional topography in the upper contact surface and in the interrelationships with the hornfels above it as suggested by aspects of this survey.

Geophysical Logging in the Proposed Rapidan Compartment

We have used borehole geophysics tools to characterize some of the bulk petrophysical properties of the Coffeewood Correctional Center site at depth, including using a Mount Sopris Instruments* winch with an Advanced Logic Technologies (ALT)* OBI–40 optical televiewer (OTV) for imaging fracture geometries, and generating inventories of fracture densities. These tools and measurements include a Century* three-arm caliper, natural gamma, formation resistivity, fluid resistivity, single point (SP) and American Petroleum (AP) conductivities (via the electromagnetic induction tool), and temperature measurements, all as functions of depth. The asterisk (*) denotes a registered trademark.

The original total well field is comprised of nine wells. Three of the original nine wells are currently dedicated pumping wells and are centrally located. The five other boreholes are currently monitoring wells and surround the central group of three. Our field program has logged all five of the monitoring wells (see figs. 9 through 13), as part of this investigation with two being selected for OTV logging.

In the well numbering scheme, we have adopted the references “OBS–1”, “OBS–2”, for example, to denote the well of interest within the field. These correspond to the first and second observation wells, respectively, within the series. This scheme, in turn, correlates with a numbering system adopted by the original site engineers (MMM Design Group, Inc.) in collaboration with the commercial groundwater consulting company charged with site evaluation (Emery & Garrett Groundwater, Inc., 1992). The specific correlations are: OBS–1 = MMM–E; OBS–2 = MMM–A; OBS–3 = MMM–B; OBS–4 = MMM–F; and OBS–5 = MMM–4. The progression from OBS–1 through OBS–5 moves from west to east across the Coffeewood facility. See figure AIII-3, for a well access site map.

The bedrock geology at the Coffeewood facility (see figure 5B) consists of hornfels (after Balls Bluff Member siltstone) overlying the Rapidan diabase lopolith. From a regional perspective, the Rapidan hydrodynamic compartment is thus a lens-like inlier of hornfels cradled in the concave-up upper surface of the diabase itself. The compartment is thus unconfined above, but it is everywhere confined laterally due to the presence of the surrounding low permeability diabase. With respect to the Coffeewood site, however, the hornfels rests conformably on the diabase, dipping to the north, but thinning considerably to the south and southeast. Two of the wells at Coffeewood have had a history of artesian flow. The Coffeewood wells are all collared in hornfels and OBS–1,–2, and –3 are entirely in hornfels for their total depths. Wells OBS–4 and –5, however, bottom within the Rapidan diabase lopolith. The transition from hornfels above to diabase below is particularly notable in the natural gamma logs. Well OBS–5, for example, shows a complete disappearance of natural gamma counts at the 107.5 m depth level. This is interpreted to mark the first appearance of diabase, due to the expectation of negligible amounts of Th-232, U-238 and K-40 in diabase. Similarly, the natural gamma log in well OBS–4 shows a total drop off in natural gamma counts at 82.6 m depth, and again this drop off is interpreted as the hornfels-diabase contact zone. Collateral support for this interpretation comes from the abundance of hydrothermal veins in well OBS–5, which are suggested to include, among other mineralogies, calcite. Marked increases in the calcite vein frequency occur between the 72 and 104 m depth levels but die out dramatically above 70 m (see the OTV log). We suggest that this vein distribution is due to the hydrothermal alteration patterns immediately above the diabase heat source. As such, the veins appear to have recorded the pathways of convective paleo-flow. The intersection of the diabase contact in two of the boreholes is insufficient to constrain a local contact dip (assuming planarity), however the contact with the diabase dips towards the north at about 10-15 degrees based on earlier studies (Emery & Garrett Groundwater, Inc., 1992). The horizontal separation between wells OBS–5 and OBS–4 is about 1,828 m and, after reconcilliation of the differing elevations of the well casing tops, the depth of the diabase-hornfels contact is about 17 m deeper in well OBS–5 than in OBS–4. We seriously doubt that a shallow intrusive contact such as this is actually planar, but anticipate instead, small-scale undulations in the upper contact topography.

In some sections, the hornfels is massively fractured, as is evident on the OTV and three-arm caliper logs, and these fractures are inferred to provide the 3-D fracture network required to move groundwater in the lower portions of the Rapidan compartment. Early EGGI well testing (May, 1992) as part of the Coffeewood site design has identified the hydrodynamic characteristics and groundwater-producing horizons associated with each well. The most telling pumping test—from a compartmentalization perspective—relates to the performance of well OBS–4 (MMM-F). Pumping in well MMM–2 (not one of our experiment wells) during May, 1992, induced significant drawdown in well OBS–4 (MMM–F). This is due, primarily, to the close proximity of well OBS–4 to the diabase—tantamount to the developing cone of depression impinging on a no-flow internal boundary at depth. Dipping (and thickening) regionally to the north, the hornfels thins considerably in the vicinity of well OBS–4. The permeable hornfels rock column above the diabase in this well is a scant 82 m in thickness, and thus would be expected to have a relatively limited total storage capacity. We regard the borehole measurements and observations at the Coffeewood site as very consistent with a compartmentalized flow relationship between the metamorphosed Balls Bluff Member siltstone and the diabase beneath.

The U.S. Geological Survey National Center and the Structural Eastern Margin of the Culpeper Basin

The U.S. Geological Survey (USGS) National Center rests on the eastern margin of the Culpeper basin. The 105-acre National Center campus is bisected by the margin contact,

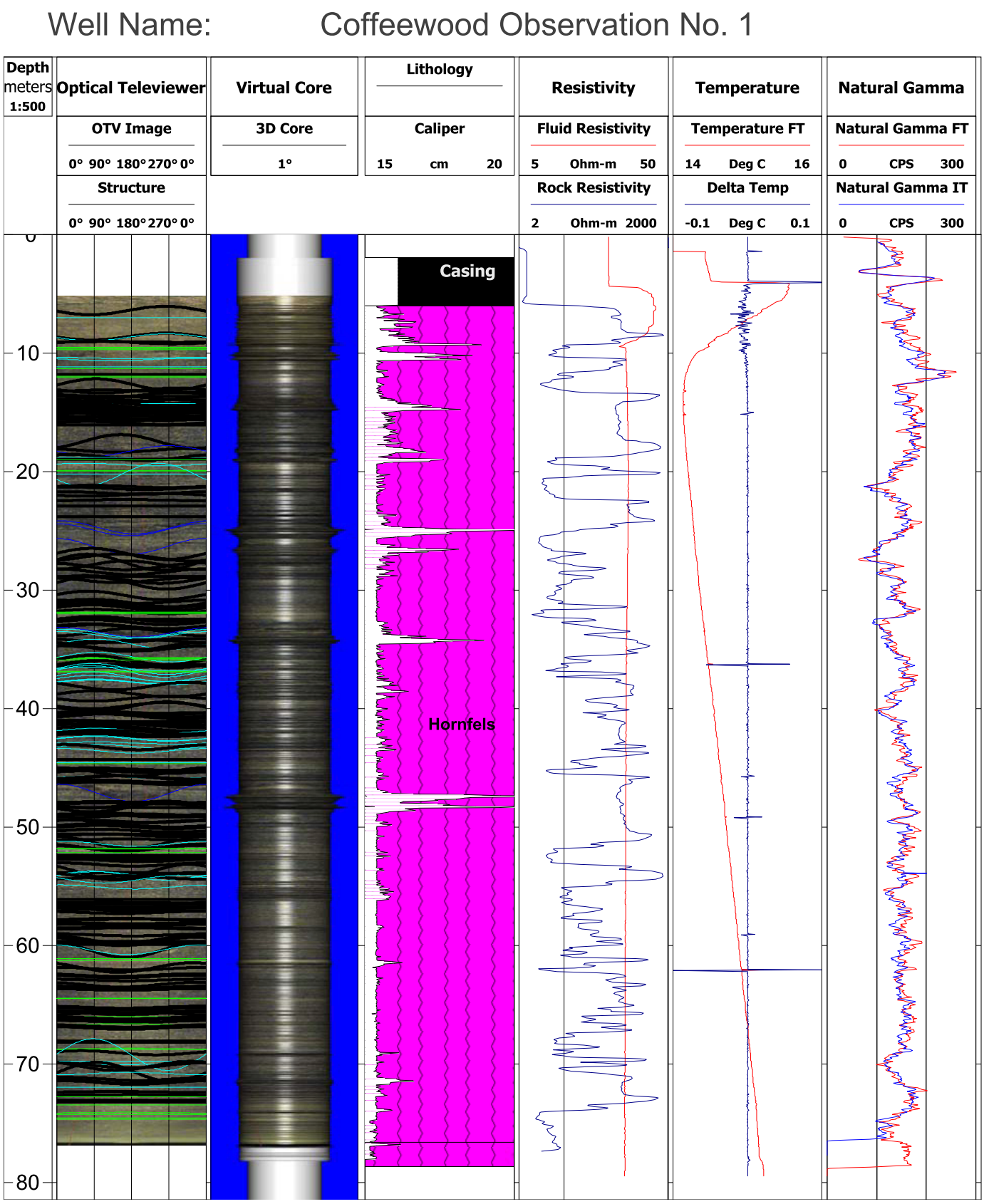

Figure 9. Geophysical logs from Coffeewood Observation well No. 1 in hornfels above the Rapidan diabase lopolith.

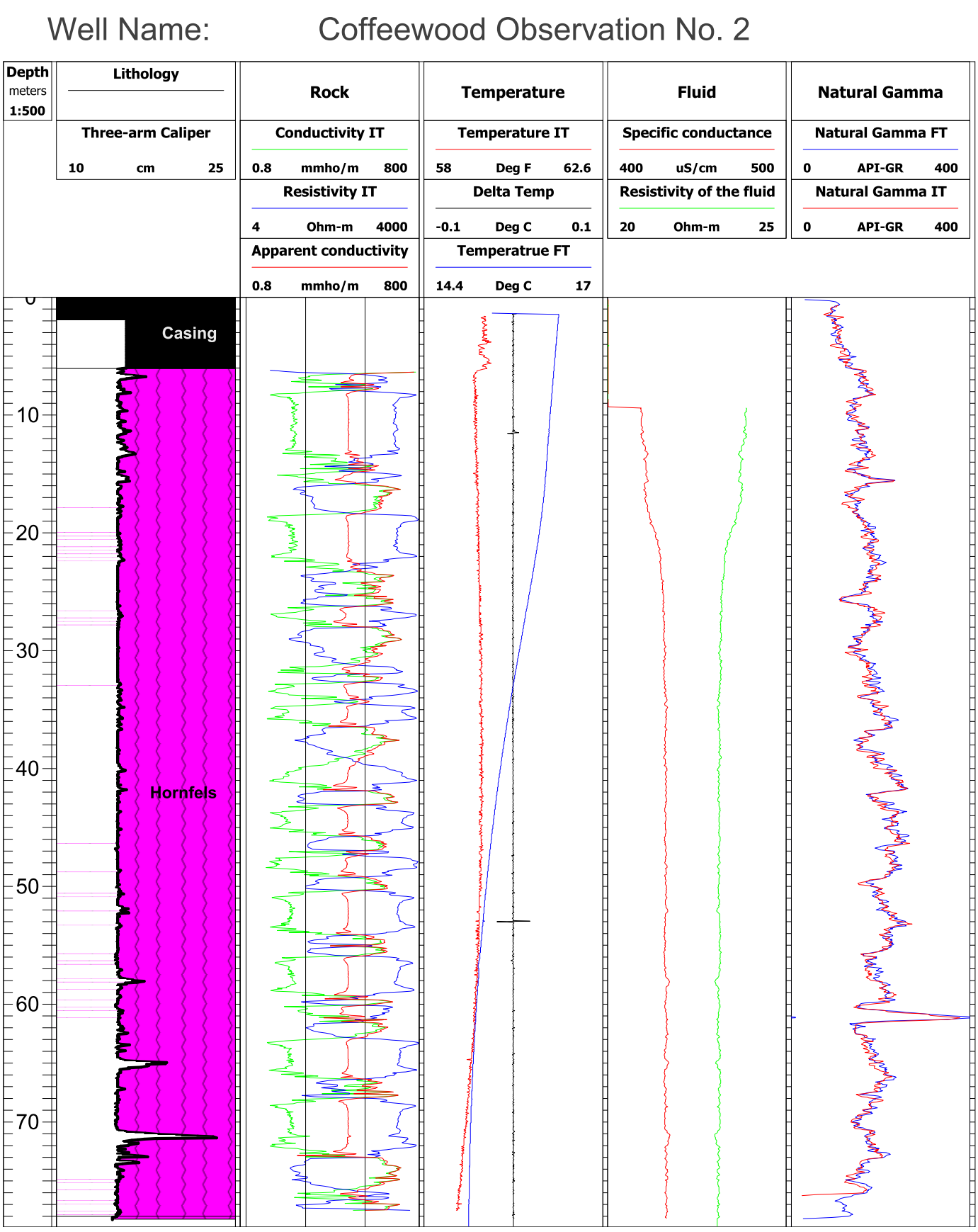

Figure 10. Geophysical logs from Coffeewood Observation well No. 2 in hornfels above the Rapidan diabase lopolith.

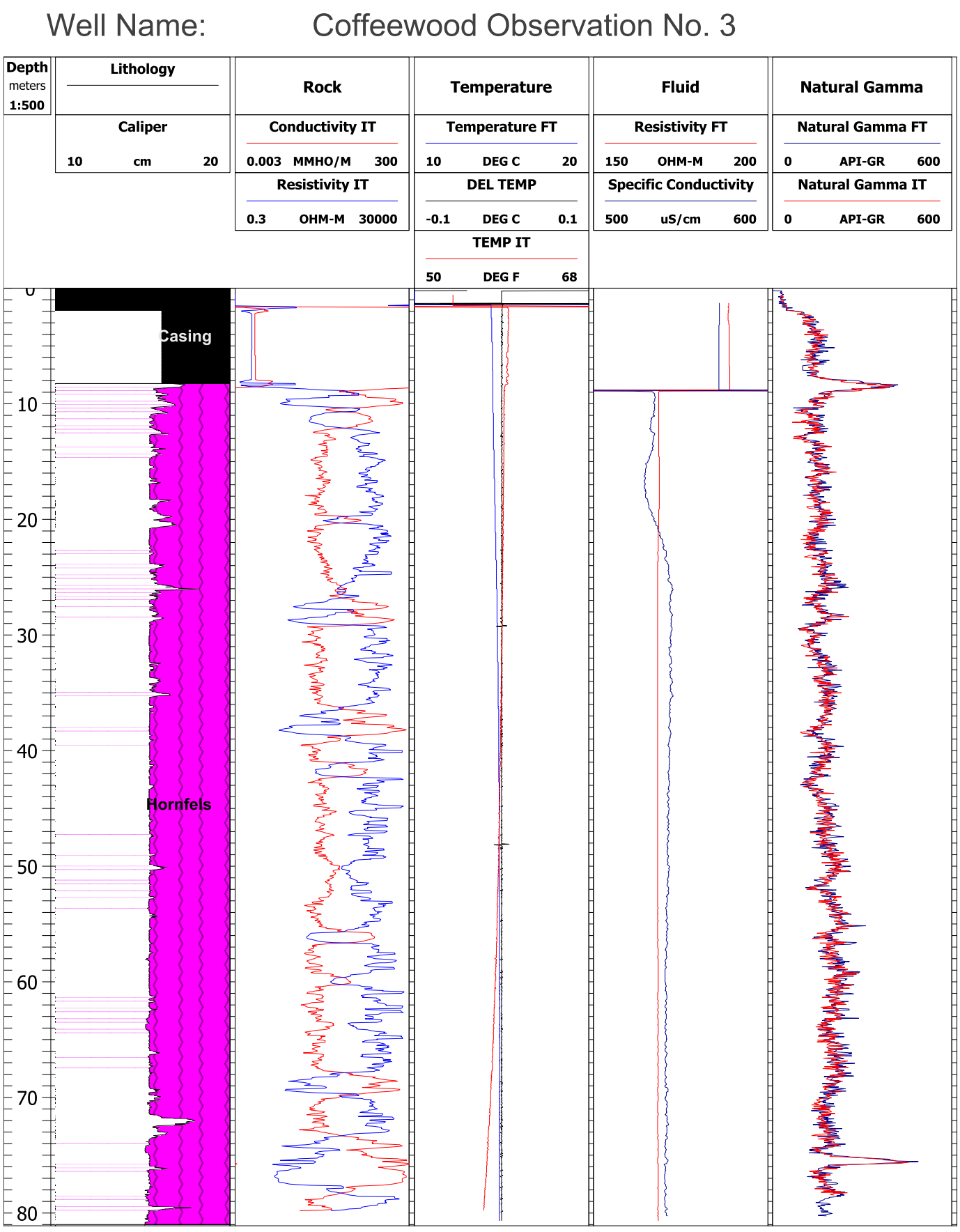

Figure 11. Geophysical logs from Coffeewood Observation well No. 3 in hornfels above the Rapidan diabase lopolith.

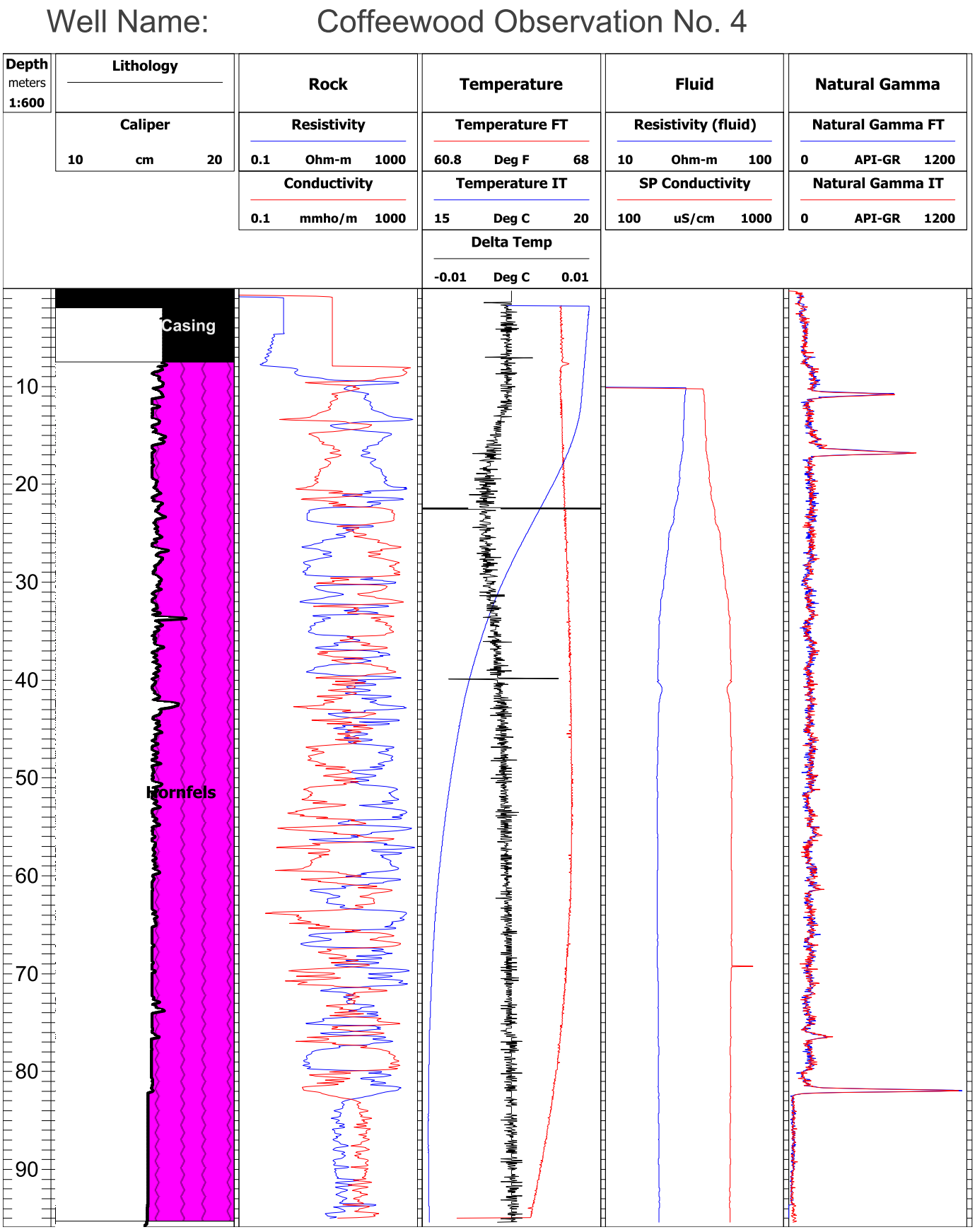

Figure 12. Geophysical logs from Coffeewood Observation well No. 4 in hornfels above the Rapidan diabase lopolith.

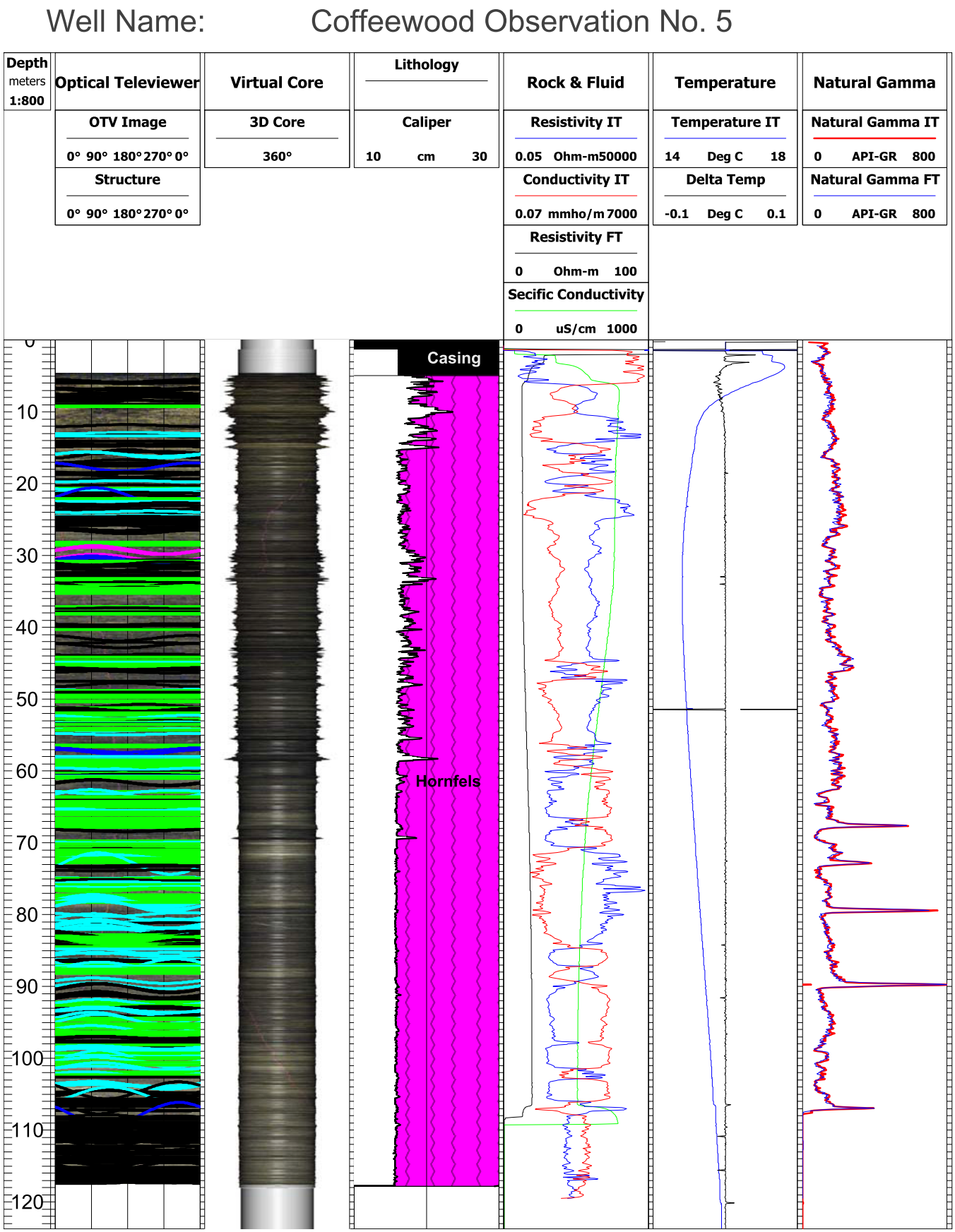

Figure 13. Geophysical logs from Coffeewood Observation well No. 5 in hornfels above the Rapidan diabase lopolith.

with the Triassaic siltstones, sandstones, and conglomerates of the basin to the west and northwest, and the late Precambrian and early Paleozoic pelitic shists to the south and east. Beneath the Center, the basin-basement contact and sediments dip about 10 degrees to the west. Interbedded sandstones and siltstones make up the Triassic Manassas Sandstone, and these grade downwards into the conglomerate of the Reston Conglomerate. The Reston Conglomerate lies unconformably on the partially weathered schists of the underlying Proterozoic basement.

Two observation wells were drilled in 1976 near Sunrise Valley Drive in Reston, Virginia for groundwater monitoring and for borehole geophysics equipment trials and tests (figure 5A). These wells are designated #52V–1D (10 inch casing; northernmost well; nearest Sunrise Valley Drive) drilled to 50.3 m and #52V–2D (8 inch casing; southernmost well; collared within a dedicated permanent monitoring house) and drilled to 62.5 m. Both wells have penetrated the basin-basement contact into Proterozoic rocks. Well #52V–1D penetrated the basement contact zone between 38.1 and 44.2 m depth. The casing of both wells extends to about 10.6 m. Open hole water levels are typically 2.5 to 3.65 m beneath the land surface.

We have conducted reconnaissance borehole geophysical surveys of well 52V–1D, using standard Century* three-arm caliper, natural gamma, formation resistivity, fluid resistivity, single point (SP) and American Petroleum (AP) conductivities (with the electromagnetic induction conductivity tool), and temperature monitoring as functions of depth (see figure 14). In addition, a RAAX* BIPS optical televiewer system was used to examine the borehole walls for structural and lithologic information. The caliper logging indicates several zones of rapid hole widening, consistent with the encounter of dilatant bedding plane fractures and/or other subhorizontal jointing and minor faults. These fracture zones occur in both the sandstone-siltstone sequence of the Manassas Sandstone, as well as in the lower conglomerate of the Reston Conglomerate. Prior flow testing (Larson, 1978) suggests that the well produces at about 1 to 5 g.p.m., a flow rate sufficient for a single family dwelling. Prior pumping tests (Larson, 1978) have indicated a transmissivity of 30-38 ft^2/day [230-290 gallons/day/foot] with a storage coefficient of 3-6 x 10^{-6}. The asterisk (*) denotes a registered trademark.

The characteristics of well 52V–2D include a transmissivity of 44 x 10^{-4} to 47 x 10^{-5} ft^2/day [330-350 gallons/day/foot], and a storativity of 1 x 10^{-4} to 6 x 10^{-5}. This greater transmissivity and storativity is consistent with the larger volume of Manassas Sandstone penetrated by this well, and attests to the important role played by the Manassas Sandstone bedding planes and cross-bedding joints in both moving and storing groundwater.

Well log data from the National Center are organized in a five column format (figure 15). Small differences from well to well correspond to the availability of either acoustic TeleViewer (ATV) data (well 52V–1D) or to heat-pulse flowmeter data (well 52V–2D). For well 52V–2D: In column 1, an ALT* OBI-40 Optical TeleViewer system was used to examine the borehole walls for lithologic and structural information. The presentation of the optical TeleViewer data follows the format used above for the Dulles and the Gainesville compartment sites. This column contains the unwrapped borehole wall lithology. In the unwrapped core, the coding for features is: (color 2-D image; orientation within core: from left-to-right vertical lines = N-E-S-W-N). Included are WellCAD (4.2) picks for the major (transmissive only) fractures (in black), mineral lineations and layering (in green), and veins (light blue); column 2 contains the virtual core. The virtual core (three dimensional color figure) depicts structures (typically fractures), mineral lineations, faults, veins, and high-angle fractures on a cylindrical surface constructed from the optical data set.; column 3 is the lithologic type (brick red = Reston Member of the Manassas Sandstone; (upper gray pebbly pattern = Conglomerate Member)); (lower gray pebble pattern = Proterozoic schist pebble conglomerate); (wavy parallel lines on green background = Proterozoic basement schist); three-arm caliper log (indentations in the lithology; and temperature (red band or red line), degrees F.); column 4 is the specific conductance (micro-Siemens/cm) and the temperature (degrees F.); column 5 contains the natural gamma counts with depth.

Used in conjunction with a Mount Sopris* heat pulse flow meter, pumping tests were conducted in well 52V–2D on 16 March 1995. Flowmeter data were collected first without pumping, to identify ambient flow conditions in the borehole. Then flowmeter measurements were made under pumping conditions to identify transmissive fractures. Figure 16 presents a summary plot of ambient upflow rates as a function of depth. No ambient flow was measured in the borehole. Next, flow in the well and in the contributing fractures was stimulated by pumping at rates of about 1 g.p.m., and the heat pulse flow meter was used to determine the locations of significant additional inflow and the correlative fracture flow rates. Figure 16 summarizes the ambient (blue curve on right-hand-side) and pumped flow rates induced by somewhat variable rate pumping (red curve on left-hand-side). The summary results for the 52V–2D pumping flow experiment are provided in figure 16, where the three depth levels contributing significant shifts to yet higher upflow rates are, in turn, correlated with influxes to the well bore from fractures at those levels.

Outcrop examination of the Manassas Sandstone, like the Balls Bluff Member siltstone, reveals that there are three primary families of joints: bedding plane fractures and a set of cross-bedding fractures that are crudely orthogonal to each other. The cross-bedding joints are, in turn, orthogonal to the bedding planes themselves (Ryan and others, 2007a), and the rock is thus orthotropic with respect to fracture permeability. These joints provide the primary porosity for fluid storage and the primary permeable pathways for fluid migration. Well 52V–2D's log depicts two fractures contributing to flow: one at about 17 m depth and another at 21 m. We tentatively interpret both of these fractures to be coincident with Manassas Sandstone bedding planes.

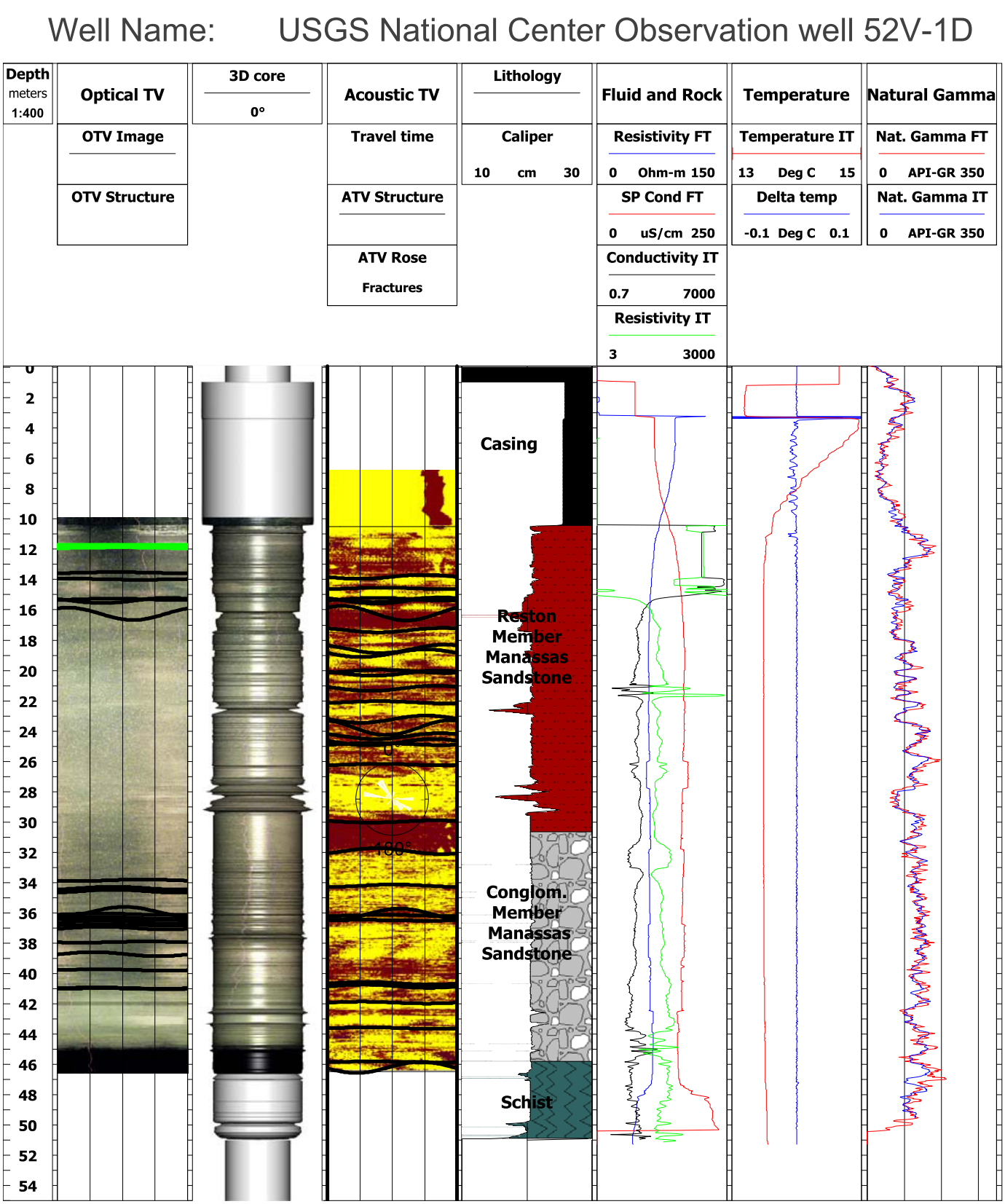

Figure 14. Geophysical logs from the extreme eastern edge of the Culpeper basin at the U.S. Geological Survey National Center observation well above the Culpeper basin basement.

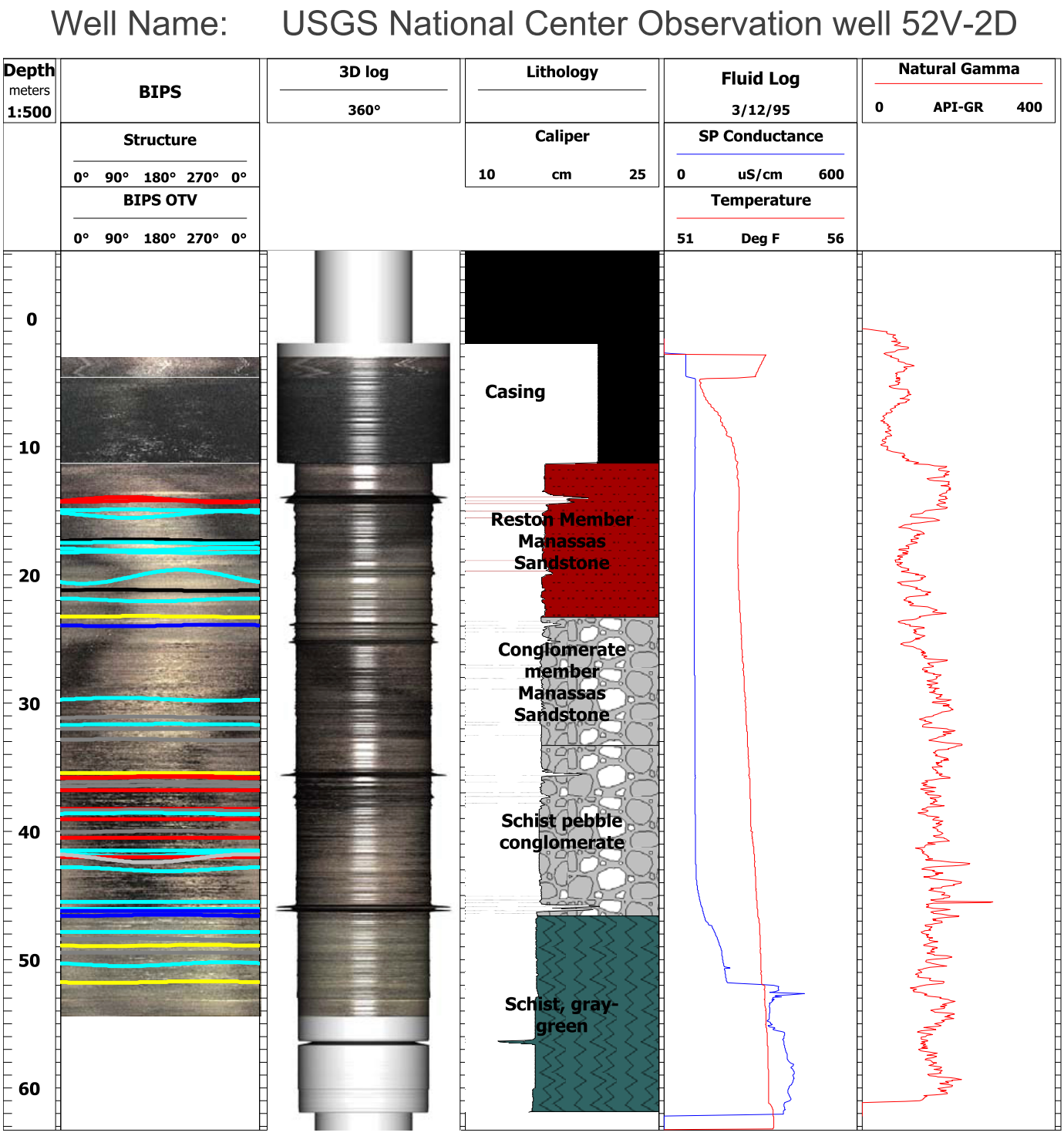

Figure 15. WellCAD logs from the USGS well 52V-2D on the U.S. Geological Survey National Center campus near Sunrise Valley Drive in Reston, Virginia.

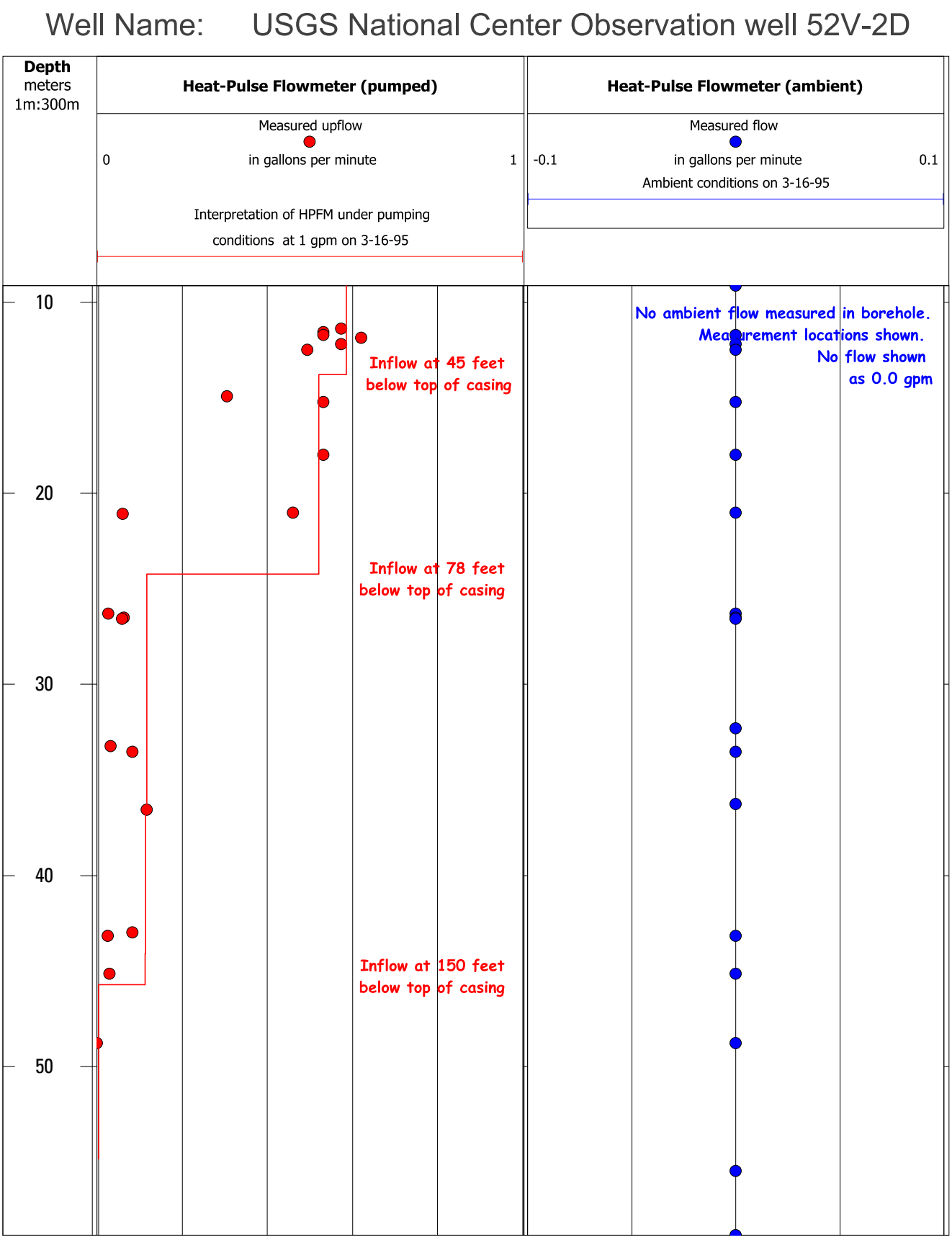

Figure 16. Heat pulse flow meter logs for USGS well 52V-2D at the National Center campus for conditions of pumping at 1 g.p.m (left plot) and for ambient (non-pumping) conditions (right plot).

Summary and Conclusions

The results of this report are both consistent with the compartmentalization concept (Ryan et al., 2007a, 2007b), and offer further elaboration of how compartments are internally structured. The principal results of individual surveys are organized on a structural basis. **The Dulles compartment.** Two wells have been logged, and both are sited wholly within the Balls Bluff Member of the Bull Run Formation. In Dulles Well No. 2 (total depth = 289 m) thirty three spikes in the first derivative of temperature with respect to depth, ($\frac{DT}{DZ}$), suggest the inflow of groundwater from a multiplicity of fractures that intersect the borehole. The spikes are unevenly distributed with depth, however they are broadly consistent with the spacing between bedding plane fractures within the Balls Bluff Member siltstone. **The Gainesville compartment.** Direct drilling has been conducted through the Gainesville diabase sheet into the subjacent hornfels (thermally metamorphosed after Balls Bluff Member siltstone). The diabase-hornfels interface (at a depth of 183 m) represents a basal flow regime where the hornfels comprises the permeable top of the Gainesville compartment confined by the diabase above. Total hole depth is 226 m. Optical TeleViewer (OTV) logging reveals that the transition from diabase to hornfels is characterized by moderate fracturing within the diabase to a massively fractured hornfels. Pumped flow rates within the diabase are ~2 gallons per minute (gpm), whereas flow rates within the hornfels at the compartment top are ~110+ gpm. These results offer further evidence supporting the (basal) compartmentalization concept. **The Rapidan compartment.** Five boreholes at the Coffeewood Correctional Center near Mitchells, Virginia have been logged to determine the relationships between the hornfels (thermally metamorphosed after Balls Bluff Member siltstone) and the diabase beneath. The transition from hornfels to diabase is particularly notable in the natural gamma counts where, in well OBS–5, a complete disappearance of gamma counts occurs at a depth of 107.5 m. Marked increases occur in the calcite vein frequency between 72 and 104 m, but calcite veins die out dramatically above 70 m, suggesting that the bottom 32 m of hornfels immediately above the diabase experienced hydrothermal circulation during the cooling of the lopolith. Pre-logging pumping tests conducted in well OBS–4 proximal to the underlying Rapidan diabase lopolith induced exceptional drawdown suggesting the presence of a low permeabilty barrier (the diabase). These results are entirely consistent with—and can be best explained by—the compartmentalization of Rapidan fluids. **The structural eastern margin of the Culpeper basin**. The eastern edge of the basin displays an on-lap relationship between the Poolesville Member of the Manassas Sandstone and the Proterozoic basement schists. The basin-basement contact and the overlying sediments dip about 10 degrees westward. Interbedded sandstones and siltstones comprise the Triassic Manassas Sandstone, and these grade downwards into the conglomerate of the Reston Conglomerate at the base of the Manassas Sandstone). The Reston Conglomerate lies unconformably on the partially weathered Proterozoic schists of the underlying basement. In well 52V–2D, pumping tests induced inflow to the well bore from three separate depth levels resulting in a net upward flow polarity for the well. Sites of inflow have been correlated with bedding plane fractures within the Manassas Sandstone. This well has a transmissivity, T, of 44 x 10^{-4} to 47 x 10^{-5} ft^2/day and a storativity, S, of 1 x 10^{-4} to 6 x 10^{-5}.

Acknowledgments

We would like to thank the several individuals and corporations that have given generously of their time and resources to make field studies, in-situ experiments and monitoring on their properties, and/or liason with their staff possible. We acknowledge Robert Cohen and Charles Faust of HIS-Geotrans Co., Sterling, Virginia; Mark McClellan and Duane Sturgill of Groundwater Systems, Inc.; and Vince Melchior of Poole & Kent Company, Baltimore, Maryland, fluid handling contractors for America On-line Corporation's data storage center at Gainesville, Virginia.

The administrative staff and the Federal, State, county, and municipal governments and agencies who have facilitated various aspects of this work, including access to their data bases, public records, their lands, and publications: Jeff Crossman and Robert Leake of the Coffeewood Correctional Center, Virginia Department of Corrections at Mitchells, Virginia; Mark Waslo and Michael Walsh of the Metropolitan Washington Airports Authority, and the Engineering Division of Dulles International Airport, for gracious access to Dulles lands, facilities, and records. The Culpeper, Fairfax, Fauquier, Loudoun, Prince William, and Orange County governments of Virginia, are thanked for their interest, support and cooperation, as are the governments of Frederick and Montgomery Counties, Maryland.

Glen A. Rubis of the Loudoun County Department of Building and Development, Leesburg, Virginia, served as a guide to contractors reports and assisted materially in the compilation of groundwater data bases for Loudoun county. David Nelms and Gary Sperian of the Richmond District of the Water Resources Discipline of the U.S. Geological Survey are cordially thanked for generously sharing resources and advice at several stages of this work, as are John Williams and Alton Anderson of the Troy, New York office of the Water Resources Discipline. Kevin Knutsen of the Branch of Geophysics of the USGS Office of Ground Water assisted in the collection of data at the USGS National Center.

Rama Kotra has provided administrative, financial and other resource support within the Eastern Region of the Survey`s Geologic Discipline. Debbie Colley, Donna Johnstone, Bonnie Jackson, Marylin Lane, and Holly Wilson have all provided helpful administrative support.

J. Wright Horton, Jr. and David L. Daniels provided perceptive and helpful reviews of an earlier version of the

manuscript that lead to improvements in the presentation. Dave Daniel's review was completed several months prior to his ultimate involvement as a coauthor. It is a pleasure to acknowledge our colleagues in the Water Resources Discipline of the U.S. Geological Survey, and we thank Carole Johnson and George Harlow for joining us in authorship. MPR thanks coauthor Carole Johnson for an exceptionally thorough and helpful coauthor review on an initial draft of the manuscript.

Patricia Packard (USGS) prepared the page layout and final text. Marci Prins (Marci Prins Professional Graphic Production, Honolulu, HI) applied her drafting skills to select figures

Century Geophysical* of Tulsa, Oklahoma, Mt. Sopris Instruments* of Golden, Colorado, Oasis Montaj* of GeoSoft Corporation*, WellCAD*, and Visual Compulog* are trade names. The use of trade names is for descriptive purposes only and does not imply endorsement by the U.S. Geological Survey, the U.S. Department of the Interior, or the U.S. Government.

Appendix I

Culpeper Basin, Virginia Borehole Tools

The borehole methods used in this survey involve several techniques for the measurement of in-situ bulk petrophysical and fluid properties. Normally, the logging equipment described here is configured with a dedicated logging truck. However, the Century Geophysical* and Mount Sopris* systems (see below) are modular and self-contained, and may be air-lifted into remote regions for specialized borehole logging operations. Asterisks (*) throughout this section denote registered trademarks.

Borehole measurements have been made in several different groundwater compartments throughout the Culpeper basin. These include composite dike- and lopolith-bounded compartments (at Dulles International Airport); lopolith-supported compartments (at Rapidan, Virginia); and diabase-confined basal-flow compartments (as at Gainesville, Virginia). In addition, we have taken preliminary measurements at the Culpeper basin's eastern margin where the juxtapostion of Mesozoic and Proterozoic lithologies has been logged. Additional discussion of logging approaches and data evaluation procedures are given in Asquith and Gibson (1983), Goldberg et al. (2002), Johnson et al. (2002), Keys (1989), Lee (1982), Luthi (2001), and Paillet and Kapucu (1989).

A combination of Century Geophysics* (Tulsa, Oklahoma) and Mount Sopris* (Golden, Colorado) tools have been used in the borehole data acquisition. The Century* system is self-contained, with the three essential components being the selected tool, the PC-Data Logger, and the winch. This system includes the Induction resistivity, natural gamma, E-log, acoustic televiewer, E-M flowmeter, and three-arm caliper tools. Similarly, the Mount Sopris* system is comprised of three primary components: the selected tool, the PC-Data Logger, and the winch. For the Mount Sopris* system, the primary tools are the Optical Televiewer and the heat-pulse flow meter. For both the Century* and the Mount Sopris* systems, tool calibrations are set through the PC control module, and most data collection and data acquisition parameters are designated via the PC interface. Nominal adjustments in the tool ascent/decent rates may be made directly on the winch. Details of tool usage at specific sites may be seen in Table 4.

Three-arm caliper. Irregularities in borehole radius and cross-sectional shape are produced by a number of factors including man-made (drilling-related) and natural causes. The intersection of fractures and fracture zones with the walls of boreholes often leads to irregularities that may be detected by the caliper tool. Thus the caliper detects relatively large and dilatant fractures that intersect the well bore. The three-arm caliper is configured with three spring-loaded arms separated by 120 degree inter-arm angles when viewed down the tool axis. Bedding plane fractures, which generally penetrate the borehole in sub-circular or elliptical sections will be crossed by all three arms of the caliper and, if of sufficient aperture, will be expressed in the caliper record as an abrupt increase in the well diameter versus depth curve. Thus the detection of fractures for the study of fracture flow is facilitated by the use of the caliper tool.

Electromagnetic Induction borehole methods. The Century* slim-hole electromagnetic induction tool contains three electrical coils. One of these coils is for transmitting an alternating current into the surrounding formation and a second coil is designated for receiving. The transmitting coil sets up a ground loop comprised of eddy currents, which in turn, set up secondary magnetic fields that induce an electrical voltage received in the upper receiving coil. This received voltage is directly proportional to the electrical conductivity of the surrounding rocks (Keys, 1989). The radius of the measurement region (zone of influence) surrounding the wellbore is, variably, 25.4 to 127 cm beyond the wellbore wall. Electrical resistivity is the inverse of electrical conductivity.

Fluid tool. This is a 'multiple sensor' tool that has several built-in capabilities, including: fluid resistivity, specific conductance, natural gamma, and temperature sensors. Specific conductance can be calculated because both the fluid resistivity probe and the temperature probe are run simultaneously allowing corrections to 25 degrees Celsius.

Optical TeleViewer (OTV). The optical televiewer combines a fixed-focus, short-focal-length camera, a light source, and a conical mirror assemblage to image the entire borehole in a 360 degree perspective. Pixelation of the images interacts with the ascent/decent rate of the tool to determine the overall image quality and resolution (see the discussion above under the specific sections related to the data derived from this tool). During data acquisition, OTV images of the borehole are displayed (unwrapped) in real time on the PC monitor in the logging truck. Typically, the data is further processed by use of WellCAD (4.2) software, where the image may be further

analyzed for lithologic, mineralogic, and structural information. The study has used a total of three optical televiewers: an Advanced Logic Technologies (ALT) OBI-40, a RAAX BIPS, and a Robertson Geologging OTV.

Acoustic TeleViewer (ATV). The acoustic televiewer is comprised of an ultrasonic transducer that both transmits and receives acoustic waves. The transmitter rotates several times per second and emits short bursts of ultrasonic pulses. The pulses transit the borehole fluid (water) and are reflected off the borehole wall. Returning to the tool, the acoustic pulses are then received by the transducer. Two measurements are made by the ATV: the total (two-way) travel time of the ultrasonic wave, and the amplitude of the reflected signal (Luthi, 2001). The televiewer digitizes 256 measurements around the borehole at each depth (DZ) interval (0.005 meters). The data is referenced to true North and then displayed using Visual Compu-Log* software or WellCAD (4.2). Because the transducer is rotating at the same time the tool is being either lowered or raised in the borehole, the actual data acquisition pathway is spiral in geometry. For each 'scan' the data is pixilated to the depth interval. During data acquisition, images of the borehole's acoustic signature are displayed (unwrapped and oriented) in real time on the PC logging monitor.

The acoustic reflection coefficient, R, is a function of the summed products and differences of the densities (ρ) and compressional wave velocities (*V*) of the borehole fluid (subscript '1') and the borehole walls (subscript '2')

$$R = \frac{\rho_2 V_2 - \rho_1 V_1}{\rho_2 V_2 + \rho_1 V_1}$$

where the product ρV is referred to as the acoustic impedance. The acoustic impedance of water is 1.5 and sandstone is 9.0 Mrayl ($kg \cdot m^{-2} \cdot S^{-1}$). In ATV records, areas of poor energy return such as fractures and cavities within the well bore wall appear as dark lines, dark bands and dark 'welts', and contrast sharply with the surrounding bright regions of higher acoustic impedance such as competent wall rock. Also, impedance may show differences in rock types and travel times will reflect enlargements in the borehole. In practice, two acoustic calipers, continuous temperature, 3-axis magnetometers and 2-axis accelleration sensors for deviation are also recorded during downhole data acquisition.

Natural gamma radiation: The Century* Slim-Hole induction tool. Natural gamma ray logging determines the total counts of Gamma emissions related to thorium, uranium and potassium—three naturally radioactive elements. The concentrations are typically detected through measurements using a NaI(Tl) scintillation counter, oriented along the borehole tool. The geochemistry of the naturally occurring radioactive elements with respect to the mineral species that they form common associations with include: (i) for Thorium [Th-232 series]: Monazite; (ii) for Uranium [U-238 series]: clays, organic phosphates and monazite; and (iii) for Potassium [K-40]: orthoclase, muscovite, biotite, evaporites and illite. The emission of natural gamma radiation from Th, U or K in association with various clay minerals has lead to the general use of the tool as a 'shale indicator' (Luthi, 2001). The volume of clay, V_{cl}, is given by

$$V_{cl} = c \cdot \frac{GR - GR_{min}}{GR_{max} - GR_{max}}$$

where GR is the gamma ray reading in the depth interval of focus, the coefficient c accounts for the relative abundance of clay in shales (a percentage factor, usually about 0.6), and the max-min notations refer to a shale (maximum clay content) and a clay-free lithology (minimum clay content), respectively. In the context of the present study, while the inferred clay content of the siltstone units varied, the most salient aspect of the variable gamma counts are the virtually complete lack of emissions in diabase bodies.

Fracture flow monitoring and measurement. A Mount Sopris* heat pulse flow meter has been used to determine the flow rates from discrete fractures. In principle, the heart of the flow meter is a pair of thermistors that are symmetrically mounted along the tool axis above and below a fluid heater grid. A rubber diaphram near the heater grid and between the entry ports seal the well bore from fluid-tool bypass, insuring that all water moves through the tool after entering one of the two fluid intakes. The direction of flow may be, of course, either upward or downward. The closure of a heating element circuit thermally 'tags' the parcel of water in proximity to the heater, which then flows along the tool axis until passing either the upper or lower thermistors. Measuring when the parcel passes and which thermistor is passed, and knowing what the separations are between heater and sensor—in combination with the tool inside diameter—makes the determination of both the flow direction and flow rate possible.

Appendix II

Locations of Culpeper Basin Wells for the Geophysical Borehole Survey

In table AII-1, the wells correspond to specific compartments within the Culpeper basin. These are, in order of discussion within the text: the Dulles compartment; the Gainesville compartment; and the Rapidan compartment. The final structural region discussed is the eastern margin of the basin at the U.S. Geological Survey National Center. In the Table, the entries corresponding to these compartments are, respectively, for the Dulles compartment: "Dulles #2 and #3"; for the Gainesville compartment: "AOL Gainesville"; for the Rapidan Compartment: "Coffeewood"; and for the eastern structural margin of the basin: "National Center".

Table AII-1. Locations and drilling data for Culpeper basin and wells.

Well	Latitude	Long	UTME	UTMN	GPS elev.	Case dia.	Drilled depth	Log depth	Water depth	Date
National Center 52V-1D	38.95125	-77.36627	294942	4313822		0.25		47.5	3.14	1/23/2001
National Center 52V-2D	38.94879	-77.3667	294900	4313550						
Dulles #2	38.94235	-77.33686	287466	4312768	106.4	0.33	291	278	7.1	1/10/2001
Dulles #3	38.93194	-77.43645	288008	4311860	109.7	0.2	313.9	41.4		1/10/2001
Coffeewood #1	38.36628	-78.03282	759241	4250418	103	0.15	83.8	76.49	3.9	11/28/2000
Coffeewood #2	38.36992	-78.03177	759321	4250825	95	0.15	83.8	77	8.99	11/28/2000
Coffeewood #3	38.37278	-78.02333	760046	4251365		0.15		80	8.67	12/1/2000
Coffeewood #4	38.36831	-78.00931	761284	4250916		0.15		94.5	9.6	12/1/2000
Coffeewood #5	38.36559	-78.02879	759598	4250352	86	0.24	137.2	118	2.24	11/27/2000
AOL Gainsville	38.77644	-77.59586	274484	4295158	116	0.2	225.5	222.25	18.1	7/19/2001

Appendix III

Culpeper Basin Borehole Data Files

There are two document types that are handled by the WellCAD reader, a borehole document (with a .wcl file extension name) and a field document (with a .wcf file extension name). Both file types are included on the DVD in a directory called "Culpeper Basin Borehole Data."

To view data (.wcl or .wcf) files you will need to install the WellCAD reader (4.2) on this DVD in the directory called "WellCAD Reader" or download the free WellCAD file reader from Advanced Logic Technologies [ALT]. [URL:http://www.alt.lu]. The reader version of WellCAD included here allows you to open files, rotate the virtual core, view the logs and the data, scale, and print WellCAD files

Appendix IV

Culpeper Basin, Virginia Borehole Location Index Maps and Table: Site Access and Well Location Logistics

Maps of use in well site access are organized in this appendix (figs. AIV-1 through AIV-5). The maps are based on standard USGS 7.5 min., 1:24,000 scale topographic base maps. They include the Mitchells, Virginia area (Culpeper County, Virginia), Dulles International Airport Authority (Fairfax and Loudoun Counties, Virginia), the Gainesville America On-Line (AOL) site (Prince William County, Virginia), and the USGS National Center site (Fairfax County, Virginia). With the sole exception of the U.S. Geological Survey, all other areas that are either Federal, State of Virginia, or privately-owned and are generally closed to the public. Special permissions must be secured to gain access. The maps are presented here for completeness, and to place the wells within their cultural context.

Appendix V

A Glossary of Selected Terms

Definitions of hydrologic terms and porous media trans–port parameters may be found in Bear (1972, 1979), Dullien (1979), Strack (1999), Polubarinova-Kochina (1962), and Kovacs (1981). In certain cases, terms below may not appear within the text but are, instead, used as part of the definition of other terms that do appear.

Darcy's law: Darcy's law expresses the relationship between fluid flow and the driving forces for flow in combination with the resistive agents that oppose or retard the flow. It is quite analogous to Fourier's law of heat conduction, Fick's law of diffusion, Newton's law of viscosity, and Ohm's law in electricity. The volumetric flow rate, Q, is:

$$Q = -(kA/\eta_{shear})(\Delta P/L)$$

Where A is the cross-sectional area of the reference volume, L is the length of the reference volume, P is the piezometric head of the fluid, η_{shear} is the dynamic shear viscosity, and k is the permeability.

Dulles International Airport Authority wells (Loudoun County, Virginia)
The Dulles compartment

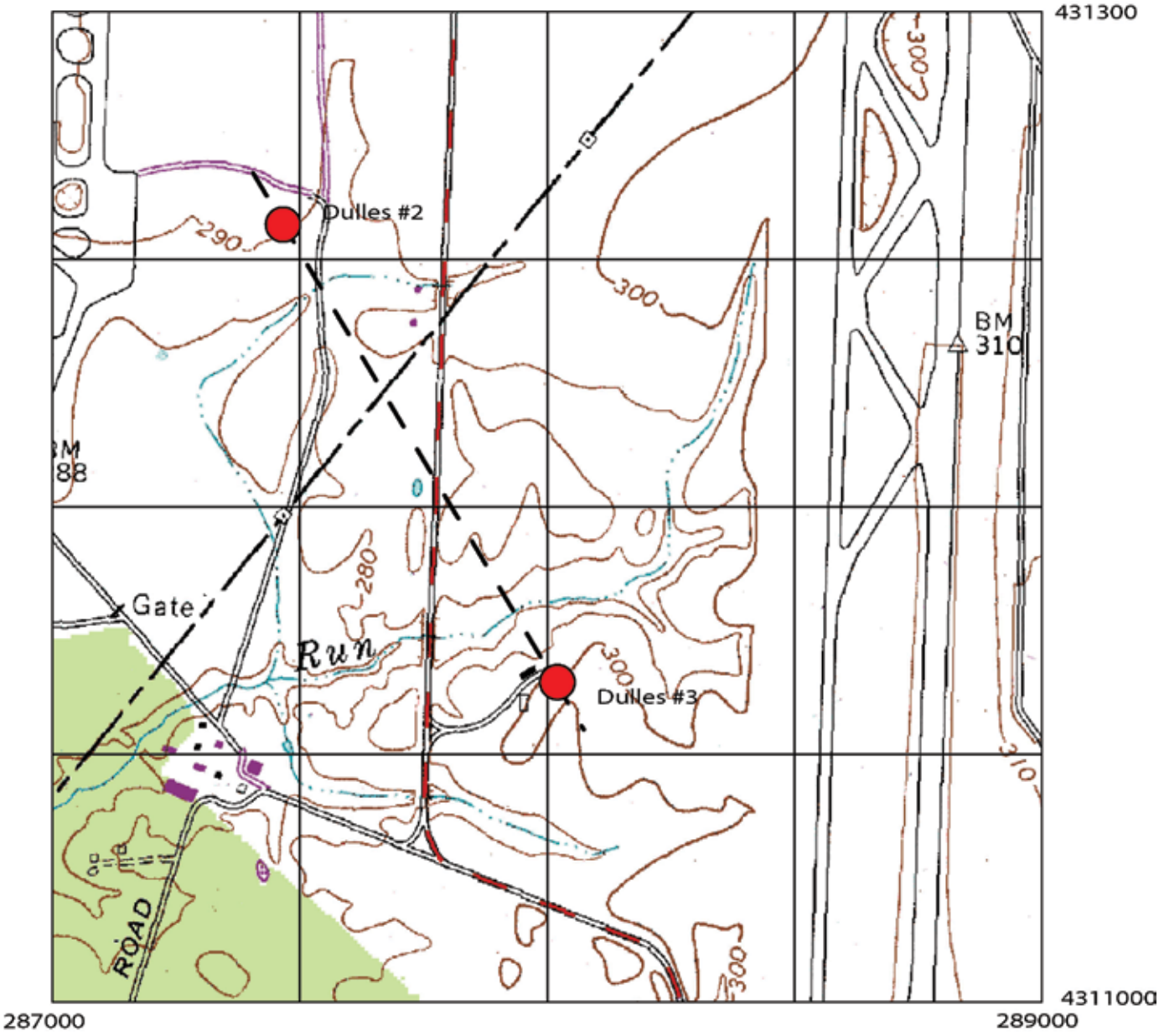

Figure AIV-1. Map showing locations of two Dulles area boreholes. The Dulles area borehole data set contains two logged wells. This map is an index to the original sites and their selection location projected onto a portion of the original 7.5 min. quadrangle map. The grid is 500 m on a side. Data for the surveys may be downloaded by clicking on: data.

Gainesville, Virginia. America On-Line (AOL) well (Prince William County, Virginia)
The Gainesville compartment

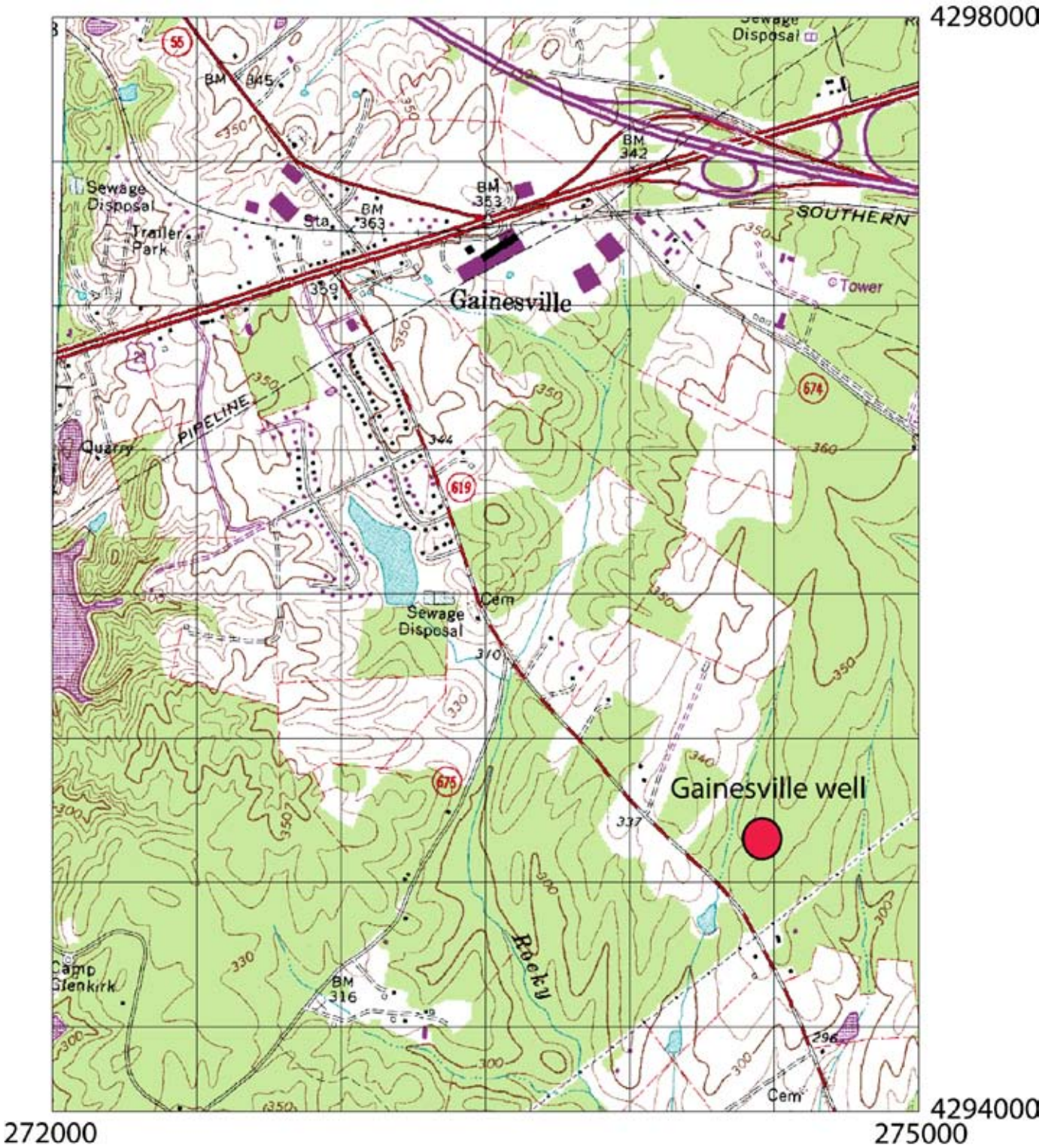

Figure AIV-2. Maps showing location of the Gainesville, Virginia, area borehole (AOL-GV-740), which was completed on America On-Line's data center site. Data for this survey may be downloaded by clicking on: data.

Mitchells, Virginia area wells (Culpeper County, Virginia)
The Rapidan compartment

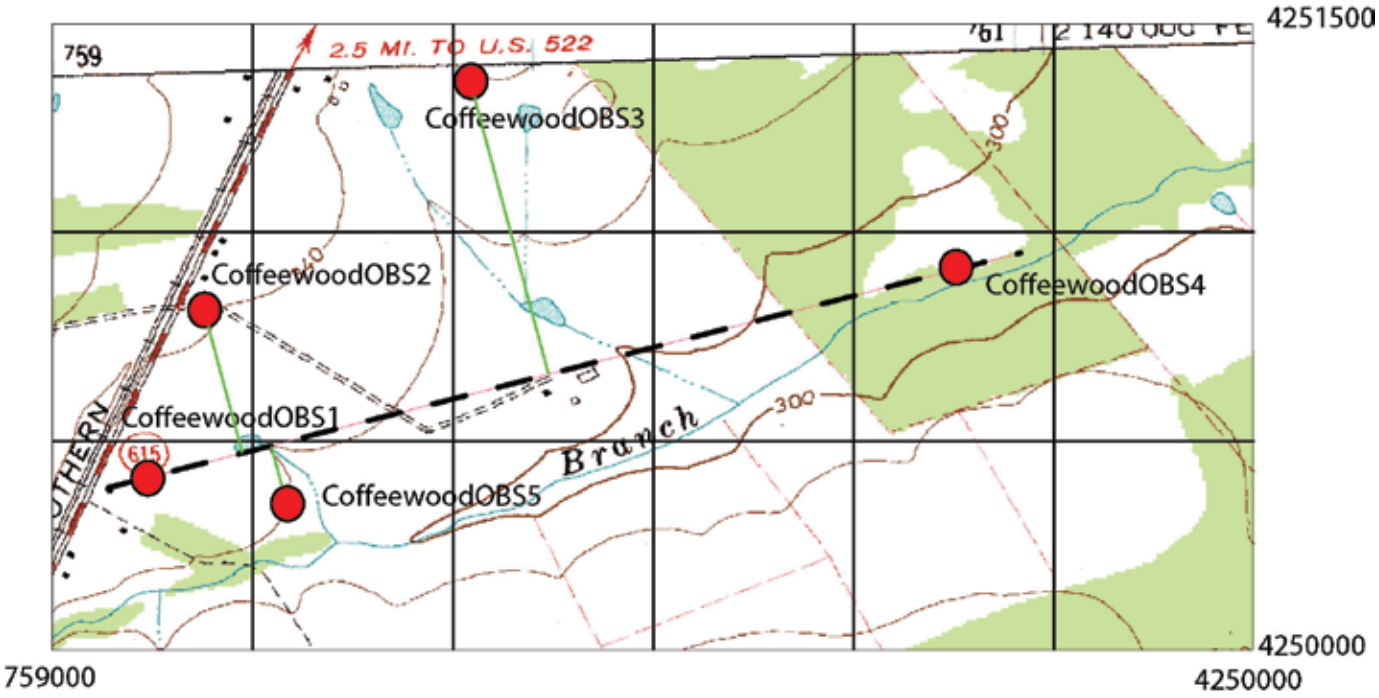

Figure AIV-3. The Mitchells area, Culpeper County, Virginia. The Coffeewood Correctional Facility property contains 5 wells that were logged in this study. Coffeewood wells OBS–1 and OBS–5 contain optical televiewer data. The location map contains the positions of the wells projected on a line. Data for the surveys may be downloaded by clicking on: data.

U.S. Geological Survey (USGS) National Center, Reston, Virginia.
Eastern structural margin of the Culpeper basin. (Fairfax County, Virginia)

Figure AIV-4. The U.S. Geological Survey National Center observation wells (52V–1D) and (52V–2D), in Reston, Virginia. These boreholes were completed on the 105-acre National Center campus and are located at the extreme eastern edge of the Culpeper basin. Data for these surveys may be downloaded by clicking on: data.

Hydraulic conductivity: The hydraulic conductivity of an aquifer is the ability of the rock mass to transport aqueous fluids under the drive provided by hydraulic gradients and resisted by the properties of the fluid. It is defined under 'permeability' below, and is symbolized as *K*.

Permeability: The permeability, *k*, may be defined in terms of the hydraulic conductivity, *K*, as:

$$K = k\gamma/\eta_{shear} = kg/\eta_{kinematic}$$

Where γ is the fluid specific weight, and , $\gamma = \rho G$ where *G* is the accelleration of gravity and ρ is the fluid density. In the permeability expression, η_{shear} and $\eta_{kinematic}$ are the dynamic shear viscosity and the kinematic viscosity, respectively. Note in particular that the expression for hydraulic conductivity contains entities that relate only to the properties of the porous medium (*k*), and entities that relate only to the properties of the fluid passing through it (γ, η_{shear}, and $\eta_{kinematic}$). The dimensions of permeability are L^2, and are usually expressed as m^2. Sometimes *k* is called the intrinsic permeability.

Piezometric head: The total of the elevation head and the pressure head is referred to as the piezometric head. The piezometric head is measured with a piezometer, or an open tube whose diameter is sufficiently large to avoid capillary effects, and screened in its lower sections to freely admit the fluids sampled. Collectively, piezometric heads measured independently over an extended region are referred to as a piezometric surface. Each measurement point within such a data group potentially contains an elevation component and a pressure component, thus the total piezometric surface must also be viewed as the conceptual sum of a elevation surface and a pressure surface.

Storativity: The storativity (*S*) of a body is defined as the volume of fluid released from (or taken into) the body (of unit horizontal cross-section) per unit decline (or rise) in the piezometric head. Alternately, it may be viewed as the volume of fluid added to the body under conditions promoting a decrease (or increase) of the piezometric head. Storativity is also referred to as the coefficient of storage.

Transmissivity: The transmissivity (*T*) of a body indicates an aquifers ability to transmit fluid through its entire thickness, *h*. The formation transmissivity is the product of the hydraulic conductivity (*K*) and the aquifer thickness. The parameter is dimensionless.

$$T=Kh$$

For example, basal flow beneath confining diabase sheets and lopoliths may occur within the underlying hornfels and within the deeper sandstone/siltstone sequence, and these units may act collectively as an aquifer transmitting groundwater horizontally. Transmissivity is an indirect measure of fluid properties through its component hydraulic conductivity.

References Cited

Asquith, G. B. and C.R. Gibson, 1983, Basic Well Log Analysis for Geologists. Methods in Exploration Series. American Association of Petroleum Geologists. 216 p.

Bear, J., 1972, Dynamics of Fluids in Porous Media. Dover Publications. New York. 764 p.

Bear, J., 1979, Hydraulics of Groundwater. McGraw-Hill International Book Company, New York., New York. 567p.

Cohen, R., 2001, Review of America On-Line (AOL) Gainesville pump test. [prepared for the Poole & Kent, Corporation, Baltimore, Maryland]. I GeoTrans, Inc., Sterling, Virginia. 6p.

Çoruh, C., Bollinger, G.A., and Costain, J.K., 1988, Seismogenic structures in the central Virginia seismic zone, Geology, v. 16, p. 748-751.

Drake, A.A., Jr., and Lee, K.Y., 1989, Geologic map of the Vienna Quadrangle, Fairfax County, Virginia and Montgomery County, Maryland: U.S. Geological Survey Geologic Quadrangle Map GQ-1670, scale 1:24,000, one sheet.

Dullien, F.A.L., 1979, Porous Media: Fluid transport and Pore Structure. Academic Press. New York, New York. 396 p.

Emery and Garrett Groundwater, Inc., 1992, Hydrogeologic report. Results of groundwater exploration and development program. Phases I-V. (for) Virginia Department of Corrections. Deep Meadow Prototype IV. VDOC-MSD Facility. Submitted to: MMM Design Group; Virginia Department of Corrections. Virginia Department of Health. Vol. I & II. Appendices A-F.

Faill, R.T., 2003, The early Mesozoic Birdsboro central Atlantic margin basin in the Mid-Atlantic region, eastern United States. Geological Society of America Bulletin. V. 115, 406-421.

Froelich, A.J., 1982, Map showing the mineral resources of the Culpeper basin, Virginia and Maryland: Availability and planning for future needs: Miscellaneous Investigations Series Map (1:125,000). Map I-1313-B.

Froelich, A.J., 1985, Map and geotechnical properties of surface materials of the Culpeper basin and vicinity, Virginia and Maryland: Miscellaneous Investigations Series Map (1:125,000). Map I-1313-E.

Goldberg, D.S., D.J. Reynolds, C.F. Williams, W.K. Witte, P.E. Olsen, and D.V. Kent, 2002, Well logging results from the Newark rift basin coring project. Scientific Drilling. Springer-Verlag,URL:*http://www.ldgo.columbia.edu/BRG/RESEARCH_PROJECTS/NEWARK/PUBLICATIONS*, Pp. 1- 9.

Johnson, C.D., F.P. Haeni, J.W. Lane, Jr., and E.A. White, 2002, Borehole-geophysical investigation of the University of Connecticut landfill, Storrs, Connecticut: U.S. Geological Survey Water-Resources Investigations Report 01-4033. 187 p.

Keys, W. Scott, 1989, Borehole geophysics applied to groundwater investigations. National Ground Water Association. 313 p.

Kovacs, G., 1981, Seepage Hydraulics. Elsevier Scientific Publishing Company. Amsterdam. 730 p.

Laczniak, R.J. and C. Zenone, 1985, Ground-water resources of the Culpeper basin, Virginia and Maryland: U.S. Geological Survey. Miscellaneous Investigations Series Map (1:125,000). Map I-1313-F.

Larson, J.D., 1978, Hydrogeology of the observation well site at the U.S. Geological Survey National Center, Reston, Virginia: U.S. Geological Survey Open File Report 78-144. 29 p.

Lee, J., 1982, Well Testing. Society of Petroleum Engineers. New York, New York and Dallas, Texas. 159 p.

Lee, K.Y., and Froelich, A.J., 1989, Triassic-Jurassic stratigraphy of the Culpeper and Barboursville basins, Virginia and Maryland: U.S. Geological Survey Professional Paper 1472: 1-52 p.

Luthi, S.M., 2001, Geological well logs: Their use in reservoir modeling. Springer-Verlag. Berlin. 373 p.

Paillet, F. L. and K. Kapucu, 1989, Fracture characterization and fracture-permeability estimates from geophysical logs in the Mirror Lake watershed, New Hampshire. U.S. Geological Survey Investigations Report 89-4058. 49 p.

Pierce, H.A. and M.P. Ryan, 2003, Audio-Magnetotelluric data from the Culpeper Basin of Loudoun, Fauquier, Fairfax, Prince William, Culpeper and Orange Counties, Virginia:. A web site and CD-ROM for distribution of data. U.S. Geological Survey Open File Report 03-56. [URL:http://www.usgs.gov/pubs/ + CD-ROM].

Polubarinova-Kochina, 1962, Theory of Ground Water Movement. Princeton University Press. Princeton, New Jersey. 613 p.

Ryan, M.P., 1987, Elasticity and contractancy of Hawaiian olivine tholeiite and its role in the stability and structural evolution of sub-caldera magma reservoirs and volcanic rift systems. In Decker, R.W., Wright, T.L. and Stauffer, P.H., (eds.), Volcanism in Hawaii: U.S. Geol. Surv. Prof. Paper 1350, v. 2, p. 1395-1448.

Ryan, M.P. and J. Yang, 1999, Fracture-dominated hydrothermal convection; EOS Transactions of the American Geophysical Union, San Francisco, California; Fall Annual Meeting Program. 80, No.46, p.F-1099.

Ryan, M.P., J. Yang, and R.N. Edwards, 1997, Dike-forming intrusions and hydrothermal circulation in compartmentalized volcanic systems: Evolutionary patterns in internal porous media convection and external heat flow; EOS Transactions of the American Geophysical Union. Fall Annual Meeting. San Francisco, California., Fall Meeting Program p.F-765.

Ryan, M.P., D.L. Daniels, J.P. Smoot, A.J. Froelich, and B.D. Levy, 2000, On the geological and geophysical framework of Eastern North American Mesozoic basin hydrology: Flow deflection and compartmentalization induced by diabase intrusions. EOS Transactions of the American Geophysical Union. Spring Annual Meeting, Washington, D.C.; Spring Meeting Program. 81, No. 19, p.S-262.

Ryan, M.P, D.M. Sutphin, D.L. Daniels, H.A. Pierce, and J.P. Smoot, 2002, Three-dimensional compartmentalization of subsurface ground water flow in eastern North American Mesozoic basins. EOS. Transactions of the American Geophysical Union. Spring Annual Meeting, Washington, D.C., Spring Meeting Program. 83, No.19, p.S-151.

Ryan, M.P., D.L. Daniels, D.M. Sutphin, H.A. Pierce, P.M. Carr, J.P. Smoot, J.A. Costain, C. Coruh, and L.E. Kearns, 2007a, (in prep.), Compartmentalization and fracture flow of crustal fluids in the Mesozoic Culpeper and Barboursville basins: Conceptual, analytic and numerical models for paleo- and contemporary flow in volcanic and non-volcanic rift zone complexes. U.S. Geological Survey. Scientific Investigations Report. 224 ms pages, 185 figures, 9 tables.

Ryan, M.P., P.M. Carr, A. Ingerov, D.L. Daniels, D.M. Sutphin, H.A. Pierce, and J.P. Smoot, 2007b, (in prep.), Solitary wave-mediated magma ascent and emplacement, Rayleigh-Taylor and Saffman-Taylor instabilities, and the dynamics of compartmentalized hydrothermal fluid flow: Application to the crustal magma conduits and intrusions of the Mesozoic basins of eastern North America. U. S. Geological Survey Professional Paper. 57 ms pages, 142 figures, 1 table.

Ryan, M.P., H.A. Pierce, A. Ingerov, G. Elliott, G. Thompson, G. Torrico, C. Finateu, Y. Avram, D.L. Daniels, D.M. Sutphin, J.P. Smoot, T. Musek, D. Fox and L. Fox, 2007c, (in prep.), Magnetotelluric (MT) surveys of the Mesozoic Culpeper basin of Virginia: Data, inversions, and structural systheses of basin cross-sectional structure and diabase intrusions. U.S. Geological Survey Open File Report. (On-Line and DVD).

Ryan, M.P., H.A. Pierce, D.L. Daniels, P.M. Carr, and D.M. Sutphin, 2007d, (in prep.), Reconnaissance AudioMagnetotelluric (AMT) surveys of the island of Hawai'i: Data and comments related to the hydrogeologic structure of saddles, rift zones, dike-induced compartmentalization and the subsurface saline-freshwater interface. 53 ms pages; 23 figures and maps. U.S. Geological Survey Open File Report.

Smoot, J.P., 1989, Fluvial and lacustrine facies of the Early Mesozoic Culpeper basin, Virginia and Maryland. Field Trip Guidebook T213. American Geophysical Union. Washington, D.C. 15 p.

Smoot, J.P., 1991, Sedimentary facies and depositional environments of early Mesozoic Newark Supergroup basins, eastern North America. Paleogeography, Paleoclimatology and paleoecology. 84, 369-423.

Strack, O.D.L., 1999, Groundwater Mechanics. Strack Consulting, Inc., North Oaks, Minnesota. 732 p.

Weems, R.E. and Olsen, P.E., 1997, Synthesis and revision of groups within the Newark Supergroup, eastern North America, Geological Society of America Bulletin, v. 109, no.2, p. 195-209.